

Improving Microwave Derived Rainfall Intensities

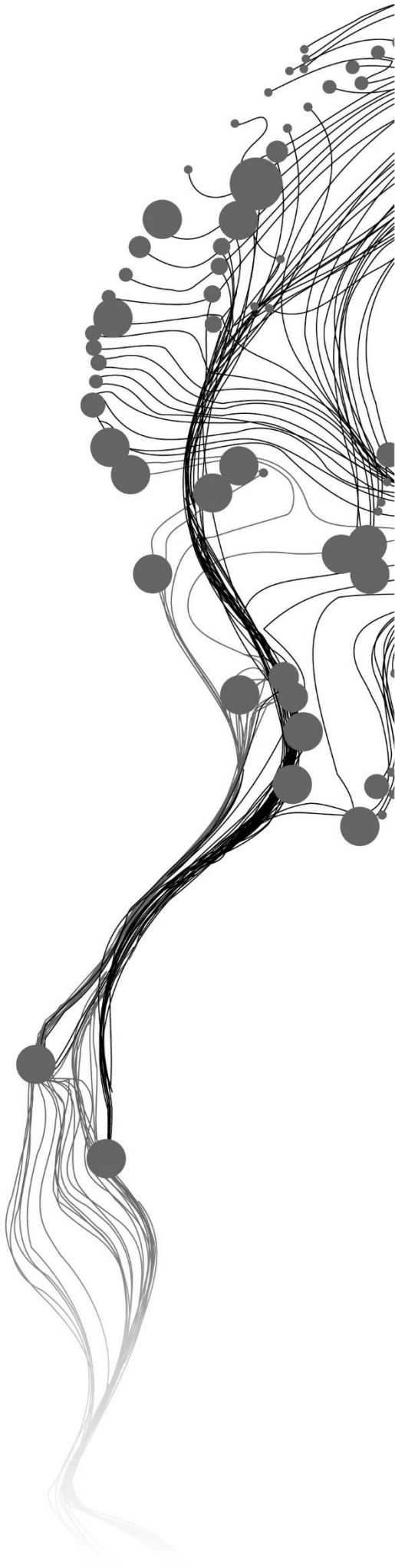
KUMAH KWABENA KINGSLEY
FEBRUARY, 2016

SUPERVISORS:

Prof. Dr. Su, Z. Bob

Dr. B.H.P. Maathuis Ben

Dr. C.B. Hoedjes Joost



IMPROVING MICROWAVE DERIVED RAINFALL INTENSITIES

[KUMAH KWABENA KINGSLEY]

Enschede, The Netherlands, [February, 2016]

Thesis submitted to the Faculty of Geo-Information Science and Earth Observation of the University of Twente in partial fulfilment of the requirements for the degree of Master of Science in Geo-information Science and Earth Observation.

Specialization: Water Resources and Environmental Management

SUPERVISORS:

Prof. Dr. Su, Z. Bob

Dr. B.H.P. Maathuis Ben

Dr. C.B. Hoedjes Joost

THESIS ASSESSMENT BOARD:

Dr. Ing, T.H.M, Rientjes (Chair)

Dr., H, Hidde Leijnse (External Examiner, Royal Netherlands Meteorological Institute)

DISCLAIMER

This document describes work undertaken as part of a programme of study at the Faculty of Geo-Information Science and Earth Observation of the University of Twente. All views and opinions expressed therein remain the sole responsibility of the author, and do not necessarily represent those of the Faculty.

ABSTRACT

Effective estimation of rainfall is significant for water resource management, hydrology, meteorology, and agriculture. Already existing rainfall estimation techniques are limited in terms of either spatiotemporal resolution or its accuracy. Signal attenuations from microwave (MW) links is known to give good estimates of rain rates. In this study, MW link signals from a single 15 GHz link in Western Kenya is used to retrieve rain rates and compared with cloud cover condition for the period rain was observed by the MW link.

The power law relation between MW signal attenuation and rain was used to estimate rain rates using 3 different coefficients: JT, LP and ITU at 15 minutes resolution. Cloud convectivity (indicating cloud cover condition) was determined at the same temporal resolution as the signal information using cloud microphysical properties (CRE, COT and CTT) derived from geostationary satellite data. Eventually, the relation between MW link derived rain rates and cloud cover conditions for the period when rain was observed by the MW link is inferred with the aim of improving the retrieved rain intensities at high temporal resolution

The performance of MW link based rainfall approach is comparable to similar studies done for the African region for similar rain type. Probability of detection is high (over 80% on the average) and modelled rain rates had on the average a coefficient of correlation, r of 0.8 and coefficient of determination, r^2 of 0.7. Cloud convectivity, signifying rain bearing clouds, seems to have quite a promising relation with the ground based rainfall observation from the MW link. The results show that such a relation has the potential to be used for upscaling the MW link derived rain rates. The procedure and the results obtained are presented and discussed.

ACKNOWLEDGEMENTS

Foremost, thanks be to God for making this whole career possible; strength did not really add much.

I would also like to express my sincere gratitude to my supervisors; Prof. Dr. Z. Bob Su, Dr. B.H.P. Maathuis and Dr. J.C.B. Hoedjes for their support, patience, enthusiasm and immense knowledge throughout my research and thesis write up. Besides my supervisor, I would also like to thank Dr. ir. Aart Overeem of Wageningen UR for his insightful comments and questions during my thesis write up. Many thanks also goes to drs. Petra Budde of ITC for her time and support in acquisition of satellite data, and Donald T. Rwasoka for his support in this study. I would also like to acknowledge SAFARICOM for providing us with microwave link data.

Although I have dedicated a lot efforts throughout my study here in ITC, it would not have been possible without the support of my friends; Aristotle Boitey, Peter N. Mahama, Mujeeb R. Nuhu and all the Ghanaian community as well as Emmanuel Kisendi, Amos Tabalia and Sammy Njuki. I would like to express my sincere thanks to them all.

Last but not least, I must express my profound gratitude to my parents, especially my mum, for their unfailing support, encouragement and prayers throughout my MSc program.

TABLE OF CONTENTS

Abstract.....	i
Acknowledgements.....	ii
Table of contents.....	iii
List of figures.....	iv
List of tables.....	v
List of equations.....	vi
Abbreviations.....	vii
1. INTRODUCTION.....	1
1.1. Research problem.....	3
1.2. Research objective.....	3
1.3. Research questions.....	4
1.4. Research hypothesis.....	4
2. LITERATURE REVIEW.....	5
2.1. Past and current application of MW signal attenuation due to rain drops for rain observation.....	5
2.2. MSG based Cloud analysis for rainfall observation.....	7
3. MATERIALS AND METHOD.....	9
3.1. Datasets: ground measurements and remote sensing.....	9
3.2. Distribution of MW links in study area.....	10
3.3. Experimental setup: ground measurements.....	12
3.4. Methodology adopted.....	14
3.4.1. Deriving rainfall intensity from MW link.....	15
3.4.2. Verifying the relation between MW link derived rainfall and cloud cover condition.....	19
4. EXPERIMENTAL RESULTS.....	24
4.1. Comparing MW link rainfall estimates to PAR from rain gauges under link transect.....	24
4.1.1. Estimating wet antenna correction factor.....	25
4.2. Correlation between link rain estimates and MSG cloud microphysical properties.....	27
4.3. Combining cloud microphysical properties for detecting potential precipitating clouds.....	31
4.4. Validation results.....	33
4.4.1. MW link rainfall estimation.....	33
4.4.2. Relation between MW link rain and cloud microphysical properties.....	34
4.5. Error analysis.....	36
5. DISCUSSION.....	39
5.1. Rainfall retrieval algorithm based on MW link attenuation.....	39
5.2. Relation between MW link rain estimates and MSG derived cloud microphysical properties.....	41
6. CONCLUSION AND RECOMMENDATION.....	43
6.1. Conclusion.....	43
6.2. Recommendation.....	44
References.....	45
Appendix.....	50

LIST OF FIGURES

Figure 1 Distribution of SAFARICOM MW links in Kericho.....	11
Figure 2 Distribution of SAFARICOM MW links in Naivasha.....	11
Figure 3 Rain gauge set up under link transect in Kericho	12
Figure 4 Rain gauge set up in Naivasha.....	12
Figure 5 Location of Microwave link transect in parallax corrected MSG image	13
Figure 6 Flowchart of methodology adapted	14
Figure 7 Relation between minimum RSL and PAR from rain gauges under link transect.....	16
Figure 8 Time series rainfall intensities recorded from rain gauges under MW link transect.....	18
Figure 9 Correlation between CTT and CTH	20
Figure 10 MSG scene not corrected for parallax effect	21
Figure 11 MSG scene corrected for parallax effect	21
Figure 12 Microwave link transect transformed to points in an MSG scene	22
Figure 13 Calibration results for MW link rainfall retrieval.....	24
Figure 14 Comparing cumulative graph of modelled and observed rain rates	26
Figure 15 Relation between MW link rain estimates and MSG IR CTT using 10.8 micron channel	27
Figure 16 Scatter plot between MW link derived rain rates and CTT_10.8 micron channel	27
Figure 17 Comparing MW link rain rates to CTT_10.8 micron channel at the early stage of cloud development.....	28
Figure 18 Comparing MW link rain rates to CTT_10.8 micron channel at the mature stage of cloud development.....	28
Figure 19 Comparing link derived rain rates to CTT_10.8 micron channel at the decaying stage of cloud development.....	29
Figure 20 Temporal variation in CRE with variation in CTT.....	29
Figure 21 Relation between CRE and COT for rainfall retrieval from clouds	30
Figure 22 Convectivity over MW link transect.....	32
Figure 23 Validation results for MW link rainfall retrieval.....	33
Figure 24 Relation between MW link rain estimates and IR CTT using 10.8 micron channel	34
Figure 25 Relation between CRE and COT	35

LIST OF TABLES

Table 1 Ground based data	9
Table 2 satellite data.....	9
Table 3 Ground based data for 2015 and beyond	10
Table 4 Satellite data for 2015 and beyond experiment.....	10
Table 5 Prefactor used as reported by Olsen et al. and ITU.....	17
Table 6 Rain gauges and the approximate distances with respect to the transmitting antenna	19
Table 7 Estimated wet antenna correction factors for coefficients used.....	25
Table 8 Instances of overestimation by wet antenna and correction applied	25
Table 9 Threshold combination for detecting convectivity	31
Table 10 Statistical analysis of MW link rainfall retrieval and cloud verification results for 11 th May 2013	36
Table 11 Statistical analysis of MW link rainfall and cloud validation results for 12 th May 2013.....	37

LIST OF EQUATIONS

Equation 1 Estimating specific attenuation in dB/km	17
Equation 2 Power law relation between attenuation and rain	17
Equation 3 Estimating POD	36

ABBREVIATIONS

BTD	Brightness Temperature Difference
CPH	Cloud Phase
CTH	Cloud Top Height
CTT	Cloud Top Temperature
EM	Electromagnetic
EML	Environmental Measurement Limited
FAR	False Alarm Ratio
GSM	Global System for Mobile Communication
ITU-R	International Telecommunication Union Radiocommunications
MPEF	Meteorological Product Extraction Facility
mRSL	Minimum Received Signal Level
MSG	Meteosat Second Generation
MW Link	Microwave Link
PAR	Path Average Rainfall
POD	Probability of Detection
RSLs	Received Signal Levels
SEVIRI	Spinning Enhanced Visible and Infrared Imager
IR	Infrared

1. INTRODUCTION

Precipitation is the most important geophysical factor that establishes a relationship between the atmosphere and the earth's surface as a key factor in weather and climate processes (Roebeling & Holleman, 2009). It is the part of the water cycle that contributes water to the Earth's surface and groundwater systems (Perlman, 2014, 2015) and, effective quantification of precipitation at high spatial and temporal resolution, is relevant for management of water resources, agriculture, weather prediction, flood and climate studies (Messer et al., 2012). Estimating precipitation has developed over time from rain gauges to satellite estimation techniques. A good measurement tool enables researchers to better understand and estimate global trends, precipitation totals, variability and extremes (Strangeways, 2006).

Rain gauges and weather radars have proved to give good ground truth estimates of precipitation (Overeem et al., 2011). However, their distribution is limited and therefore collective estimates are insufficient to monitor precipitation both spatially and temporally (Messer et al., 2012). Satellite remote sensing techniques can provide solutions for these challenges, but then data still needs to be validated with ground measurements. The use of microwave links (MW links) from the commercial cellular telecommunication network have recently been suggested as a cost effective means to estimate and monitor regional precipitation at the near surface level, and to complement existing methods (Leijnse et al., 2007a; Messer et al., 2012).

Precipitation measurements using MW links is based on the fact that raindrops in the link path attenuate the electromagnetic signals transmitted from one antenna to the other (Leijnse, 2007). This attenuation is caused by scattering and absorption by rain drops, and proportionally increases with raindrop size. By measuring the signal at one end of the link, the attenuation due to rain can be obtained. The timed measurements of such attenuation can subsequently be transformed to rain rates—which, can be compared with data from other estimation methods or used to complement other rainfall measurement methods (Overeem et al., 2011). The use of such an alternative method to estimate and monitoring rainfall offers various advantages. According to Messer et al.(2012), the wide coverage of MW communication networks makes it possible to access rainfall data for areas over complex terrains that were practically not possible by other ground methods of rainfall estimation. Also, they indicated that, a MW measures at high temporal resolution and can even measure low rainfall intensities. Quite apart, MW links are considered as environmental sensor network (ESN) that offer accurate near ground atmospheric information and also serves as a vital component in understanding other environmental processes such as wind (Messer et al., 2012) and evapotranspiration (Leijnse, 2007).

Despite their potential in estimating rainfall at higher spatiotemporal resolution, the use of commercial microwave links has some inherent uncertainties. Rios et al.(2015) in their study classified such sources of uncertainties into two categories. First, errors pertaining to individual microwave link measurements such as wet antenna attenuation, sampling interval of measurement, drop size distribution, quantization of received power, etc. Second, errors associated with the spatial density of link measurement and its effect of interpolation methodology.

In spite of these errors, the approach has been thoroughly investigated over the past five to ten years and proved to produce a good estimation of rainfall (Domounia et al., 2014; Gaona et al., 2015; Leijnse et al., 2007a; Overeem et al., 2013a). The work of David et al. (2013) suggest that, deriving rainfall intensity from MW link has an increased probability of detecting single convective cells that are associated with precipitation as compared to the conventional rain gauge measurements. The study by Rahim et al. (2011) indicate that the effect of rain on terrestrial MW link signal is more noticeable for countries located in the equatorial regions where rain intensities can be higher throughout the year.

In most cases, rainfall over the tropical areas in Africa, are produced from convective cells. Studying the development of convective cells can be particularly complex since they are mostly sudden, very local and short-lived. As such, they need to be observed at high spatiotemporal resolution for precise diagnosis and forecasting as indicated by Thomas et al., (2009). Geostationary space-borne sensors are well suited for this solution to this. The optical radiometer on board Meteosat Second Generation (MSG), Spinning Enhanced Visible and Infrared Imager (SEVIRI), observes the earth-atmosphere in 12 spectral channels. The spatial resolution at nadir is 3km for 11 channels and 1km for the High Resolution Visible (HRV) channel. The temporal resolution is 15 minutes—thus providing an increased amount of spatial and temporal information (Henken et al., 2011; Schmetz et al., 2002; Thomas et al., 2009).

This study will focus to derive rainfall intensities from MW links and infer the relationship between the ground based rain observation from MW link and cloud information surrounding the foot print of the MW link.

1.1. Research problem

Obviously, the idea of using signals from telecommunication network for retrieving rainfall is an attractive approach. For instance, MW link signal information from a network of links in the study area occur at 15 minutes interval, and the dominant rainfall type in the area is convective rainfall. Hence, making it possible to study such a phenomenon both in near real time and with close proximity to the ground. The distribution of convective cells within a cloud column results in rainfall distribution that are localised to the convective cells (Simpson, 2003). The networks of rain gauges are mostly sparse, and their density is low—thus making it highly possible for rain from a single convective cell to be entirely missed by a gauge (David et al., 2013). This, coupled with their sudden and short-lived life cycle, makes it particularly difficult to monitor and accurately represent such a phenomenon spatially (Moseley et al., 2013).

The research challenge however lies in how to link the rainfall intensities and dynamics obtained from the MW links to other sources of information. In terms of rainfall monitoring, major sub-challenges are related to:

- ✓ How to combine link derived rain rates with rainfall estimates from ground truth measurements (rain gauges) to produce a more accurate spatial distribution of rain fields.
- ✓ How to relate MW link signal dynamics and its corresponding rainfall estimates to satellite based cloud information.
- ✓ How to use satellite based information to improve and regionalize MW link based rainfall estimates.

1.2. Research objective

The main objective of this study is to derive rainfall intensity using minimum received signal levels of MW links from cellular telephone network, verify and validate the relationship between the observed rain rate from MW link and cloud convectivity derived from near cloud top microphysical properties: cloud top temperature (CTT), cloud effective radius (CRE) and cloud optical thickness (COT) using operational MSG SEVIRI satellite data.

1.3. Research questions

- How can we link rainfall detected and derived from microwave link to ground truth measurements?
- Is there a relation between ground based rainfall observation and satellite derived cloud information?
- Can we relate MW link rainfall estimates to satellite derived cloud characteristics and eventual rain rates?

1.4. Research hypothesis

There is a relation between rain rates observed from MW links and satellite derived cloud properties.

2. LITERATURE REVIEW

2.1. Past and current application of MW signal attenuation due to rain drops for rain observation

The reduction in quality and strength of radio signal propagation has long been known and studied (Leijnse et al., 2007b; Messer et al., 2012), but the intention was to improve telecommunication system design and planning (Messer et al., 2008). Researchers in telecommunication industry including Hogg (1968), Olsen et al. (1978), and Semplak & Turrin, (1969) have also, for a long time, studied the physical relationship between attenuation of radio signals and rainfall. However, their prime focus was to develop a relationship between rainfall distribution and attenuation based on different climatological setting and radio frequency, so that for a rainfall distribution statistics, corresponding attenuation statistics could be predicted (Leijnse et al., 2007b). According to Olsen et al. (1978), two general approaches have been used to estimate attenuation of radio signal due to rain. A theoretical approach involving uniformly ergodic distribution of raindrops that could be either simulated as water spheres or more complex forms; and an empirical approach which is regarded as a power law relation (using coefficients a and b) between radio signal attenuation, A , and rain intensity, R . The parameters a and b in the power law relation is dependent on frequency of the MW signal, rain drop size distribution (Leijnse et al., 2007a; Ostrometzky & Messer, 2014; A. Overeem et al., 2011), MW signal polarization (ITU-R, 2005) and rain temperature (Olsen et al., 1978). This establishes a strong basis for estimating attenuation due to rainfall (Messer et al., 2012).

However, as indicated by Leijnse et al. (2007) “ what is noise in telecommunication engineering can be considered signal in the geophysical sciences”. Considering the work of, for example Atlas & Ulbrich (1977), it has been long since the information gained from the attenuation of radio signals from telecommunication network have been used to estimate path averaged rainfall intensities. Currently, researchers like Rincon & Lang (2002) have applied the two approaches described by Olsen et al. (1978) to estimate MW link signal attenuation and subsequently estimated rain rate based on both approaches. Their results suggest that path averaged rainfall estimates from raindrop size distribution have good agreement with path averaged measurements from ground observations. Perversely, the empirical approach generally overestimates measurements from rain gauges except for stratiform rain where there was consistency with rain gauge observation.

Nonetheless, other studies have focused on this empirical relations and, used it in monitoring convective rainfall, for example by David et al. (2013) and Doumounia et al. (2014).

Leijnse et al. (2007a) have explored the use of a 27 GHz microwave link in estimating path average rainfall intensity. In their study, they illustrated the negligible effect of raindrop size distribution on power law relationship—thus uncertainties due to large variations in drop size would not transform into large errors in rainfall estimation. The reason behind this observation is explained by Atlas & Ulbrich (1977). According to them, the relation between rain-induced MW signal attenuation A , and rainfall R is linear at wavelengths close to 1cm, thereby making attenuation estimates from these frequencies suitable for rain rate estimation.

Other studies have investigated the use of a network of microwave links in constructing rainfall maps. Earliest of such techniques is the work of Giuli et al. (1991). They proposed a tomographic technique in reconstructing rainfall distribution based on a network of MW links. According to them, the spatial resolution of the reconstructed rainfall distribution maps depends on the extent of the area and the number of MW links considered. The study done by Messer et al. (2008) also follows a similar concept. Their results show that a two-dimensional rainfall map generated based on the network of MW links of different lengths, frequency and geometry, had rainfall estimates at much finer pixel resolution as compared to a corresponding radar map. Also, the MW link rain estimates were in good agreement compared to rain gauge observations. Overeem et al. (2013) have also demonstrated how variations in rainfall, in both space and time, can be retrieved for an entire country based on the network of MW links. Their work demonstrates the usefulness of MW links for country-wide rainfall monitoring in near real time.

Abrajano & Okada (2012) propose a compressed sensing technique in estimating rain rate at a specific location for tropical rains, which according to them, cause large rainfall amounts within a short time over a small area. Their approach involves the use of attenuations from a network of MW links in estimating rainfall intensities for specific locations in a particular area. According to their results, based on attenuation from a network of MW links in a given area, the specific rain location can be identified with fewer errors. The approach, according to them, is also applicable to variable rain intensities, for example for light, moderate and heavy rain. Hoedjes et al. (2014) have also coupled MW link based rainfall intensities with convective cells identified in MSG images as input for flash flood modelling in near real time. According to Thomas et al. (2009), “A convective cell is a cloud producing low temperatures, and composed of two distinct regions: the actual convective part which consists of intense, coldest, vertically extended cores, and the stratiform region characterized by a more uniform texture and lighter precipitation”.

2.2. MSG based Cloud analysis for rainfall observation

The fact that SEVIRI on board MSG observes the earth in many spectral channels gives it a high potential for application in rain detection and quantification over a wide area (Thomas et al., 2009). In most cases, geostationary satellite based rainfall observation rely on infrared (IR) information from near cloud top to predict occurrence and intensity of rain rate and assigns rain or no rain to pixels that are cloudy (Thies et al., 2008). Scofield (1987) and Woodley et al. (1982) have pointed out a number of properties of rain bearing clouds based on information inferred from cloud tops. They include but not limited to these:

- 1) cloud that have cold tops produce more rain than those of warm tops in IR images
- 2) clouds that are decaying gives little or no rain
- 3) cloud tops that are increasing in temperature in IR images produces less or no rain
- 4) cloud tops that are decreasing in temperature and increasing in area coverage produces more rain than those with opposite characteristics

Based on the above properties, Vicente et al. (1998) have adopted three guidelines in identifying the various stages of development of convective systems:

- 1) initial stages of development where there is vertical updraft resulting in rapid decline in cloud top temperature (CTT) in IR images, thus implying convective systems are intensifying
- 2) matured stages of development where, most likely, vertical updraft ceases and there is no significant change in CTT with time and there is anvil development
- 3) decaying stage where there is gradual increase in temperature of cloud tops

Considering their analysis, these guidelines was used when assigning rain rate to MSG IR pixels.

Also, multispectral analysis of IR satellite data have been used to retrieve cloud physical properties including: cloud optical thickness (COT) and cloud particle effective radius (CRE), which are then used to infer the precipitation probability of clouds or compared with ground truth observation from rain gauges or weather radar (Lensky & Rosenfeld, 2005; Rosenfeld & Gutman, 1994). The results of Rosenfeld & Gutman (1994) indicate that reflectance at 3.7 channel (here in indicated as 3.9 micron channel) is much dependent on cloud drop radii. For clouds with small droplets near cloud top, they observed high reflectance at 3.7 channel, but for thick clouds composed of ice crystals near cloud top, they observed low reflectance at the 3.7 channel. Hence, implying different reflectance absorptivity response due to temporal variation in cloud phase with cloud top height. Their results indicate that the 3.7 channel is much sensitive to cloud drop distribution, hence, could be used as an indicator of CRE. They indicated that for precipitation to occur, clouds need droplets with CRE not less than 14 micrometres and CTT of less than or equal to 260 Kelvin. They also adapted spectral difference between 10 and 12 micron channel as an indicator COT; a difference of

less than 1 Kelvin implies clouds are optically thick and a difference of more 1 Kelvin implies clouds are optically thin.

Roebeling & Holleman (2009) adapted the approach described by Rosenfeld & Gutman (1994) to retrieve CRE and cloud phase (CPH) near cloud top for potential precipitating clouds, and validated the retrieval algorithm using weather radar. Rosenfeld (2007) illustrates how microphysical evolution of convective clouds can be observed based on the analysis of the CRE and CTT relation. The idea is based on the premise that cloud droplets develop at the base of clouds while growing with respect to increasing height or temperature decline. He indicated, such a dependency of CRE with temperature holds relevant information about cloud formation and precipitation process.

Quite apart, Rientjes & Alemseged (2007) and Rosenfeld (2007) have indicated that this technique is an indirect measurement technique because they observe precipitation by observing other cloud properties at the top of clouds. According to them, since IR radiations are not able to penetrate thick and opaque cloud columns, a lot of the IR radiations reaching satellite sensors are from the interaction with cloud microphysical properties near cloud top. As such the radiations have little or no interactions with the actual precipitation particles within the cloud column. Rosenfeld (2007) also indicates that precipitation can vary significantly with respect to cloud depth and composition: thus cloud particle distribution and cloud phase. The results by Rientjes & Alemseged (2007) demonstrates that, the relation between CTT and rain intensities is often weak.

This study also applies the widely known power law relationship between rain-induced microwave signal attenuation A , and rainfall intensity R , in estimating rain rate using information from a single MW link. However, unlike other approaches demonstrated by other researchers, the link derived rainfall intensity are verified with near cloud top microphysical properties derived from spectral analysis of MSG IR satellite data using the approach described by Rosenfeld & Gutman (1994). The results of such relation is validated using different rain events and cloud conditions.

3. MATERIALS AND METHOD

3.1. Datasets: ground measurements and remote sensing

There are mainly three major data used in this study:

- 1) radio signals transmitted from a transmitter on one tower to a receiver on another tower of a single (15 GHz) MW link, at 15 minutes sampling interval. This is received from a telecom company SAFARICOM, in Kenya.
- 2) time series rainfall from rain gauges
- 3) and operational MSG SEVIRI satellite data.

It is worth knowing that the prime focus of this study was to first compare and assess the relation between ground based rain observations from MW links; and based on this relation, develop an algorithm that would be used to upscale these rain observations for areas surrounding the link using thermal infrared satellite data (with day and night capabilities). In this regard, two field datasets are considered: 1) In the months of April, May, June 2013, an experiment was conducted in Kericho by Hoedjes et al. (2014). Time series rainfall data from 5 ARG 100 tipping bucket rain gauges (manufactured by EML, under license from Centre for Ecology and Hydrology, www.wittich.nl), received signal levels (RSLs) and geostationary satellite data have been obtained. Table 1 and 2 describes the details of datasets for the 2013 experiment.

Data	Temporal resolution
RSL (15GHz) (3.68km)	15 minutes
Rain gauge rainfall	1 minute

Table 1 Ground based data

Data	Date (2013)	Temporal resolution	Spatial resolution
MSG 6.2 and 10.8 (CTT)	May	15 minutes	3 x 3 km
MSG 3.9 and 12.0	May	15 minutes	3 x 3 km

Table 2 satellite data

2) During field work in the months of September and October 2015, experimental setup was established in Naivasha. Fifteen ARG 100 tipping bucket rain gauges (manufactured by EML, under license from Centre for Ecology and Hydrology, www.wittich.nl) were acquired. Nine of which were installed in two separate farms namely; Delamere (3 rain gauges installed) and Gorge farm (6 rain gauges installed) as indicated in Figure 4. The remaining 6 are to be concentrated under one MW link; although 3 have been installed so far (see Figure 4). Table 3 and 4 presents the details of the datasets for 2015 experiment and beyond.

Data	Temporal resolution
RSL (15GHz) (6.23km)	15 minutes
Rain gauge rainfall	1 minute

Table 3 Ground based data for 2015 and beyond

Data	Temporal resolution	Spatial resolution	Characteristic
(CTH) (NWC-SAF)	15 minutes	3X3km	Product assigns height values to cloud top identified in MSG pixels
CPH (NWC-SAF)	15 minutes	3X3km	Products give an indication of cloud phase for clouds identified in MSG pixels
MSG (CTT)(6.2 and 10.8 μm)	15 minutes	3X3km	6.2 and 10.8 μm channel would be used in retrieving CTT values for each cloud identified in MSG pixel.

Table 4 Satellite data for 2015 and beyond experiment

Due to delay in acquisition of signal strength data and also location of suitable spots for installing rain gauges, the later part of the focus of this study (upscaling derived rain rates) could not be met. However, the former (modelling rainfall, verifying and validating relation with cloud cover), which is also the objective of this study is carried out and its results presented. Regarding this, archived data for two days: 11th and 12th May 2013 are used. These two periods are selected on the basis of consistency of RSLs and relevant rain events that were observed. The data for 11th May 2013 is used in calibrating the rainfall retrieval algorithm based on MW link signal attenuation as well as verifying the relation with satellite derived cloud conditions. Whereas the data for 12th May 2013 is used in validating the assessed relation between MW link derived rain and cloud conditions. On the other hand, the real time data from 2015 experimental set up is intended to be used in developing the upscaling algorithm, depending on the relation established with May 2013 dataset.

3.2. Distribution of MW links in study area

Diagnostic data for signal strength are received from SAFARICOM a telecommunication company in Kenya, which operates about 3000 MW links throughout the country. This data is received in Eastern African Time (EAT) but are converted to Universal Time Coordinated (UTC) for easy intercomparison with rain gauges and satellite. In Kericho (located in Western part of Kenya), SAFARICOM operates six MW links with variable frequencies (both 15 and 23 GHz links) and link lengths.



Figure 1 Distribution of SAFARICOM MW links in Kericho

Figure 1 is a Google Earth image showing the distribution of SAFARICOM’s microwawe links in Kericho. In Figure 1, duplex links (thus they transmit and receive signals) are shown as blue pins, transmitting links and receiving links are shown as red and green pins respectively.

In Naivasha, SAFARICOM operates about 20 individual MW links with most of them located close to Lake Naivasha as shown in the Google Earth image in Figure 2.

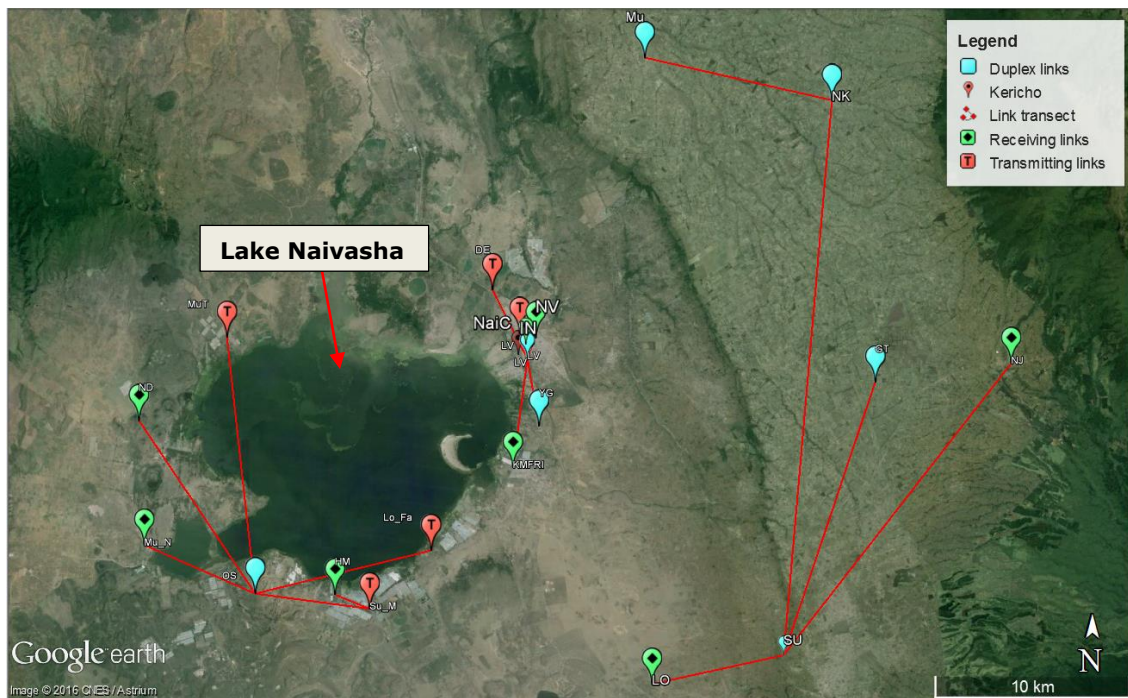


Figure 2 Distribution of SAFARICOM MW links in Naivasha

3.3. Experimental setup: ground measurements



Figure 3 Rain gauge set up under link transect in Kericho

In Figure 3 set up of rain gauges under MW link during Kericho experiment (2013) is shown. Five ARG 100 tipping bucket rain gauges (manufactured by EML, under license from Centre for Ecology and Hydrology, www.wittich.nl) were installed under a 3.68km 15GHz MW link at variable intervals.



Figure 4 Rain gauge set up in Naivasha

Figure 4 illustrates set up of rain gauges during 2015 field work. Three rain gauges are installed so far under a single 15 GHz MW link (6.23 km), located in south western part of Lake Naivasha. Further to this, 6 rain gauges were installed (distributed in northern and southern part) in Gorge farm, located to the south of Lake Naivasha and 3 in Delamere farm, located in the north eastern part of Lake Naivasha. The set up of the rain gauges is designed to capture the occurrence and spatial variability of rainfall along the MW signal transmission path and also in areas close to the link.

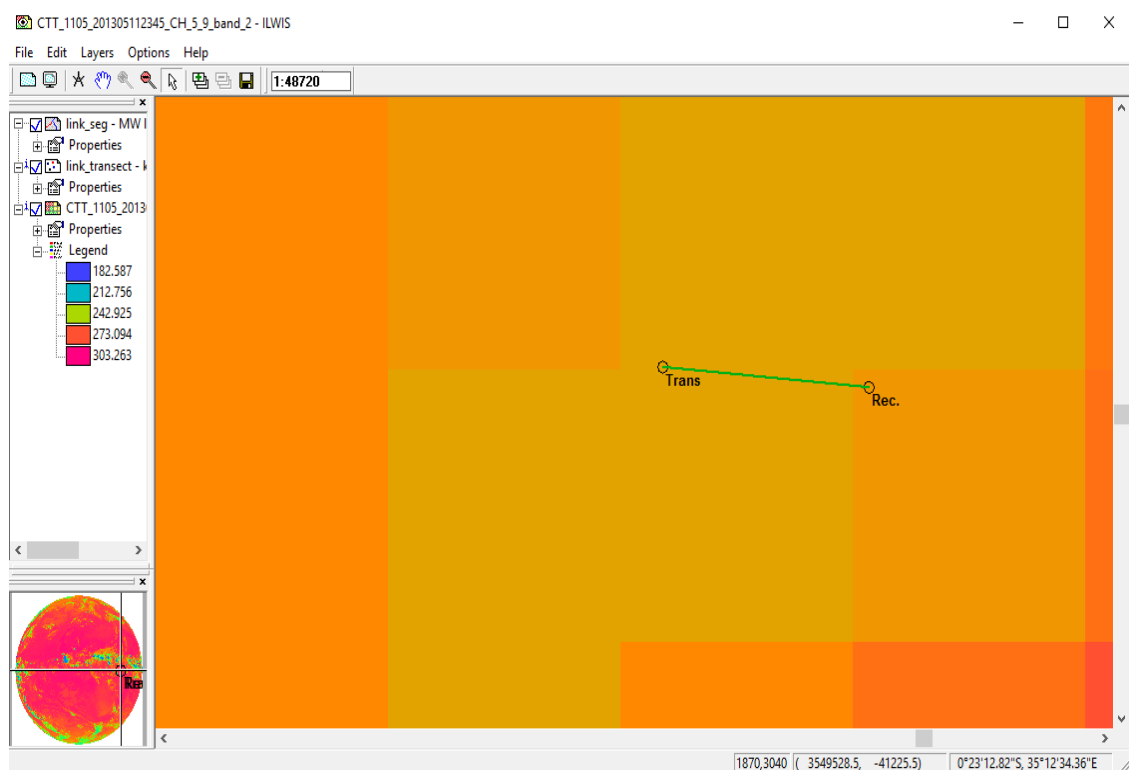


Figure 5 Location of Microwave link transect in parallax corrected MSG image

Where Trans and Rec. in image are transmitting and receiving antenna respectively. Coloured background image is MSG (IR 10.8 micron channel) scene which indicates CTT, that decrease from hot (red/orange colour in image) to cold (blue colour in image)

Figure 5 illustrates the location of the link transect within an MSG CTT scene for the period of 11th May 2013, 11:45 PM. The length of the link transect approximately falls within the area of one MSG pixel, however from Figure 5, it can be seen that link transect passes through 3 MSG pixels.

3.4. Methodology adopted

The potential of estimating rainfall intensity using microwave link cannot be overemphasized as indicated by several authors (Gaona, 2012; Kestwal et al., 2014; Wang et al., 2012). It has been long recognised that the presence of hydrometeors such as fog and rain extremely affects the propagation of microwave signals in the lower atmosphere. Increased rain rate results in increased microwave signal attenuation since electromagnetic waves are mostly affected by scattering and absorption by hydrometeors (Kestwal et al., 2014).

Figure 6 illustrates the procedure adapted for this study. The idea is similar to the one illustrated by Hoedjes et al. (2014) in terms of incorporating satellite based cloud information (cloud top temperature, CTT) with MW link based rainfall estimation. Unlike their approach, this study incorporates other satellite derived near cloud top properties like; cloud effective radius, CRE and cloud optical thickness, COT with MW link derived rainfall estimates to better infer the relationship between the two.

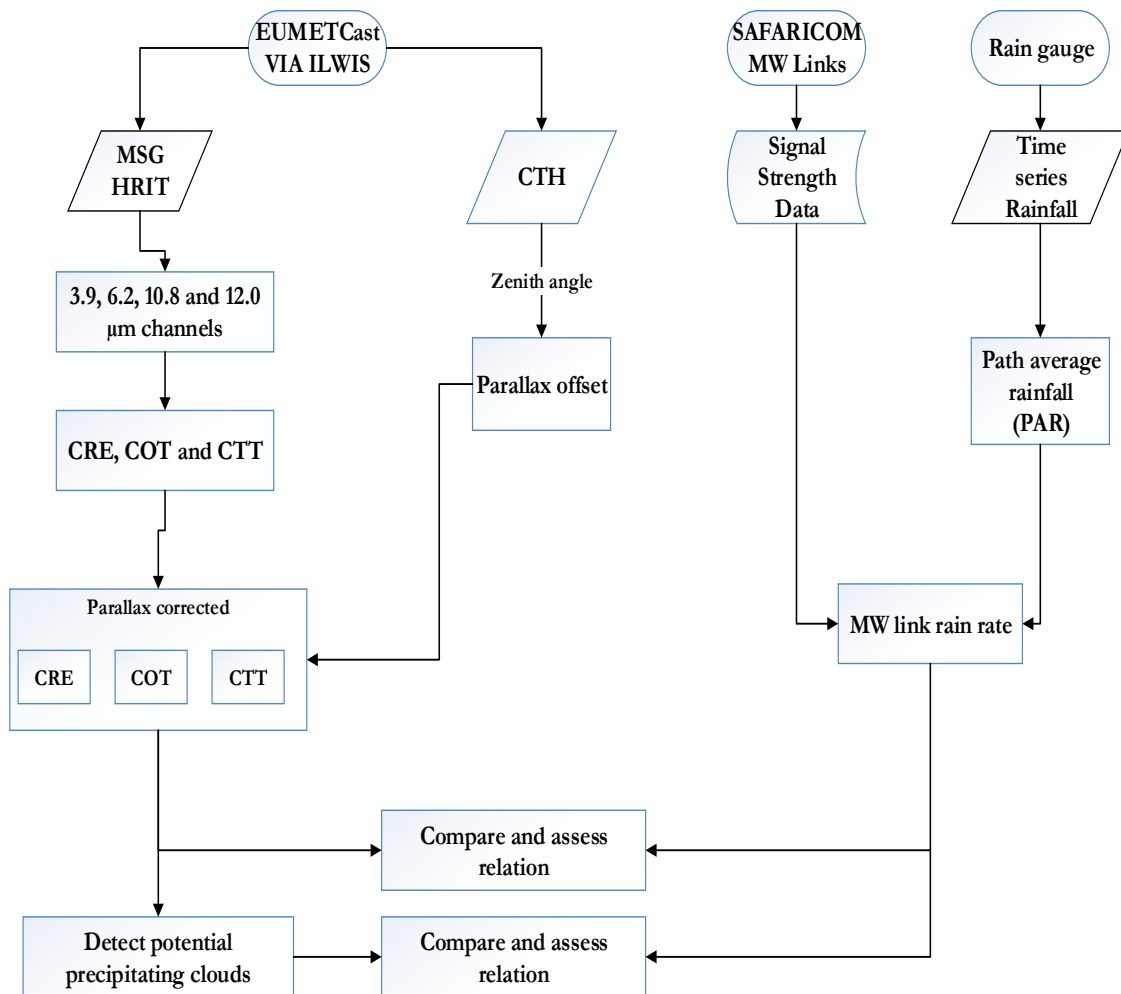


Figure 6 Flowchart of methodology adopted

An algorithm to develop rain rate fields using rain intensities derived from MW link signal strength data and MSG satellite image data has been demonstrated by Hoedjes et al. (2014). Their approach involves estimating convectivity from the evolution of convective scenes in MSG images using 6.2 and 10.8-micron channels. Before this, parallax offset and subsequent parallax correction are done based on cloud top height estimate from 10.8-micron channel of deep convective complexes. MSG pixels are then linked to MW link signals, and consequently, the estimated convectivity were then used to transform MW link derived rain intensities into rain fields. This might be error prone, because the cloud top height (CTH) estimate is computed based on standard atmospheric measurement and moist adiabatic lapse rate that in turn requires accurate meteorological measurement—which are unavailable for most of Kenya.

In the absence of enough satellite data for the estimate of a more accurate CTH for the experimental period, an approximate estimate is computed by first establishing a correlation between the CTH and CTT in near real time. The resulting relation is used to compute the CTH for the experimental period. The CTH estimate is then used to correct the images for parallax effects.

One implicit drawback of the idea of using telecommunication signals in retrieving rain intensity is that occurrence of rainfall should be within the signal transect for the rain to be detected. To account for this, the study area selected for this study has a sufficient number of MW links and so maximises the chance of detecting rainfall if it occurs.

MW link signal attenuation is not only caused by rain. Schleiss & Berne (2010) point out two random process that cause attenuation of MW link signal: attenuation due to rain and attenuation baseline (that is attenuation caused by other sources). Domounia et al., (2014) indicate other sources of attenuation, depending on the frequency of the MW link includes: changes in air refractivity, dust or technical problems such as antenna misalignment. Another well-known source is the so-called wet antenna attenuation that is caused by a film of water that settles on the antennas at the onset of rain and as such increases the attenuation along the link (Doumounia et al., 2014; Leijnse et al., 2008; Kharadly & Ross, 2004; Zinevich et al., 2010). These aspects would not be explicitly considered in detail as far as this study is concerned.

3.4.1. Deriving rainfall intensity from MW link

The exact procedure for estimating rainfall using microwave link is followed as illustrated by Hoedjes et al. (2014). The idea is to transform the maximum signal loss, indicated by the minimum RSL (mRSLs), into accumulated rain rate. This approach is valid because it has been confirmed that at heavy and moderate rainfall periods, the minimum RSLs (mRSLs) carry most of the information with respect to rainfall (Ostrometzky & Messer, 2014). In this study, signal strength data for 11th and 12th May 2013 are used. The data for 11th May 2013 are first used to calibrate link derived rain rates based on MW signal attenuation verifying the relation with cloud cover conditions derived

from MSG satellite data. The validity of the relation between MW link derived rain rates and satellite derived cloud conditions is assessed using data for 12th May 2013 and its corresponding cloud conditions.

3.4.1.1. MW link data processing

Signal strength data obtained were first cleaned and observed for consistency in signal transmission as well as its response to a rain event. Figure 7 illustrates the relation between the minimum received signal levels (mRSLs) obtained from SAFARICOM for the period 11th May 2013 and path average rain intensities (PAR) from rain gauges under link transect for the same period.

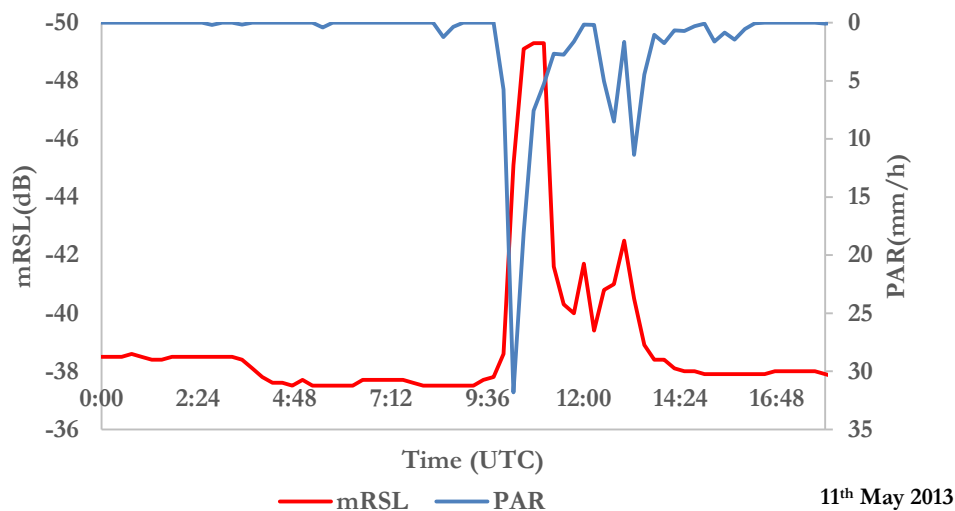


Figure 7 Relation between minimum RSL and PAR from rain gauges under link transect
Where mRSL is minimum received signal level and PAR is path average rainfall intensities from rain gauges under link transect

For the rain event that occurred on this date, there exist a strong negative correlation between the 15 minutes sampled mRSLs and observed PAR from the rain gauges under the link transect. It is also quite distinct from this relation when the links were wet and when they were not. These observations are similar to the ones reported by Doumounia et al. (2014).

The follow up step after these observations is to classify the mRSLs into wet and dry periods. For this study, the moving window variance method, a procedure described by Schleiss & Berne (2010), coupled with observations from the rain gauges are used in classifying the mRSLs into wet and dry periods. The moving windows variance classification method by Schleiss & Berne (2010) is based on how the signal varies with time (see appendix 1 for illustration). The occurrence of rain drops in the signal path results in significant and frequent drop in signal level, and so its local variance is higher than the corresponding dry period (Domounia et al., 2014). The approach was applied to a time window of ten 15 minute intervals. Schleiss & Berne (2010) described the choice of window as an important step and indicated that it is linked to the nature of rainfall under study. Considering the characteristics of rain events from convective scenes, selecting a shorter time window would be

inappropriate since such events are mostly short lived. As such, the algorithm might fail in detecting the occurrence of a rain event.

The time window used hereafter is large enough to overcome this limitation. Applying this approach results in a time series of statistical variance at every 2 hours 30 minutes which is then compared with PAR from rain gauges under link transect to identify wet and dry periods of the link. Eventually, the reference signal level which is also a time series signal level, giving an indication of the mRSLs during preceding dry period can be estimated. This was estimated based on the average of 10 preceding dry periods (the equivalent of 2 hours 30 minutes period). Attenuation due to rain is then computed by subtracting the mRSLs during the wet period from the reference signal level, and the corresponding specific attenuation, A (dB/km), is estimated based the relation in equation 1.

Equation 1 Estimating specific attenuation in dB/km

$$A = \frac{P_{ref}(L) - P(L)}{L} \quad (1)$$

$P_{ref}(L)$ and $P(L)$ correspond to reference and mRSL (dB) respectively whereas L (km) corresponds to the length of the link transect.

3.4.1.2. MW link rainfall estimation

To retrieve rain intensities from MW link signal attenuation, the widely known power law relation between signal attenuation and rainfall is used. The relation is of the form described in equation 2.

Equation 2 Power law relation between attenuation and rain

$$A = aR^b \quad (2)$$

Coefficients a , b in equation 2 depend on frequency, drop shape, drop size distribution along the path of MW transmission (Domounia et al., 2014) and rain temperature (Olsen et al., 1978). Table 5 presents that adapted values of the a and b coefficient used in this study. It can be seen that the exponents, b , are all approximately equal to 1; thus implying near linearity in equation 2. As demonstrated by Olsen et al. (1978) and Leijnse et al. (2007a), the relation in equation 2 should be less sensitive to drop size distribution (DSD).

	a	b
Laws and Parsons (LP_H)	0.0459	1.076
Joss et al. (JT)	0.0589	0.966
ITU	0.05008	1.0440

Table 5 Prefactor used as reported by Olsen et al. and ITU

The values indicated for Laws and Parsons (LP_H) and Joss et al. (JT) are reported by Olsen et al., whereas those indicated for ITU were adopted from International Telecommunication Union

Radiocommunication report P.838-3 (ITU-R, 2005). Olsen et al. (1978), derived specific attenuation values based on different drop size distributions, which are then used to estimate a and b coefficients based on different frequency, drop size distribution and temperature. The values indicated in Table 5 for JT are for thunderstorm distribution, developed from the mean drop size distribution from convective rain. Those of LP are for high rain rates and developed from drop size distribution spectrum from continental temperate rainfall. Both values indicated are for a rain temperature of 20°C and 15GHz frequency. Considering the dominant rainfall type within the study area, the adapted values although not justified, are not trivial. International Telecommunication Union-Recommendation (ITU-R) sector provides guidelines for estimating specific attenuation from rain rates. Their reported values of a and b are derived from curve fitting to power law coefficient, and estimated for different frequency and polarization. Values indicated in Table 5 are for 15GHz frequency and of vertical polarization. To identify the suitable prefactors for the rain phenomena under study, rain events that were observed on 11th May 2013 were modelled using the different coefficients, in Table 5, using the relation in equation 2 (see appendix 2 for illustration).

Rain intensities were monitored at 1 minute interval using 5 rain gauges under link transect but aggregated to 15 minutes interval and used to estimate Path Average Rainfall (PAR) intensities. The procedure for PAR involves averaging the observed rainfall from each gauge based on their proximity to either an antenna (receiver or transmitting) or to its nearest working neighbor and or proximity to the link transect (Leijnse et al., 2007a).

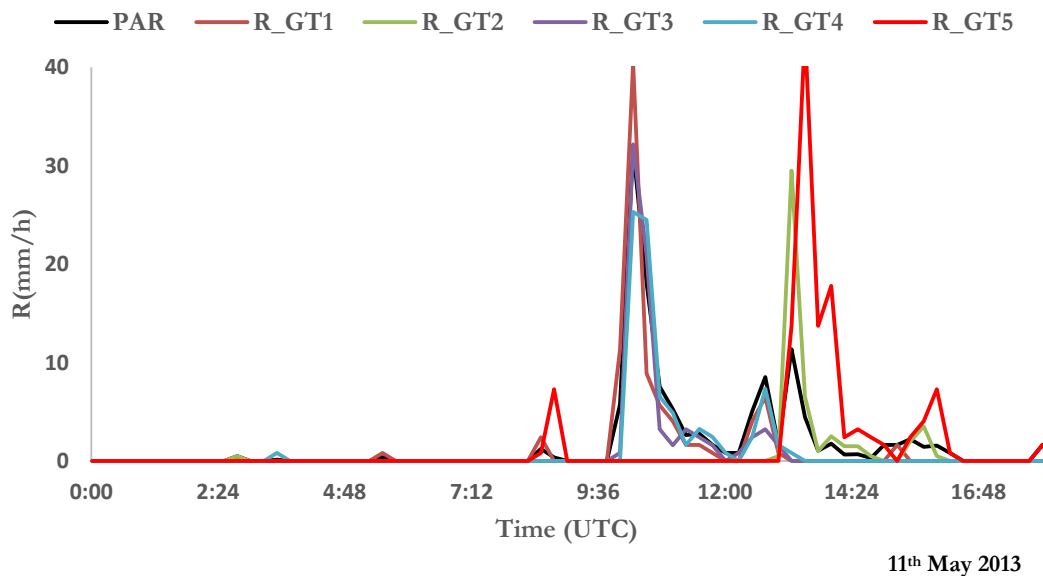


Figure 8 Time series rainfall intensities recorded from rain gauges under MW link transect. Rain gauge estimates of 5 gauges that were installed under link transect, for the experimental period, 11th May 2013. Where R_GT is rain gauge under link transect, and PAR is path average rain rate for gauges under link transect.

Figure 8 and Table 6 compares the rainfall intensities that was recorded from the five rain gauges under the link transect and the approximate distances of each of the rain gauges under the link transect with respect to the transmitter, respectively. It can be seen from Figure 8 that there is high spatial and temporal variability in the observed rainfall from each gauges even at considerably short distances as shown in Table 6.

Gauge	Distance from Transmitter (km)
1 (R_GT1)	3.74
2 (R_GT2)	2.96
3 (R_GT3)	1.99
4 (R_GT4)	1.35
5 (R_GT5)	0.38

Table 6 Rain gauges and the approximate distances with respect to the transmitting antenna

Eventually, the PAR might not always represent a true average of the point measurements from the rain gauges as was also indicated by Leijnse et al. (2007). The MW link rainfall estimates based on different coefficients are then compared with the PAR.

3.4.2. Verifying the relation between MW link derived rainfall and cloud cover condition

Generally there is a robust relation between cold cloud top and observed rain rates (Rosenfeld, 2007) as has also been observed by several authors including: Hanna et al., (2008), Scofield (1987) and Vicente et al. (1998). To verify if there is a relation with the observed rain rates from the MW link and the cloud cover condition for the experimental period, the approach illustrated by Rosenfeld & Gutman (1994) is used. This involves multispectral analysis of IR satellite data to retrieve microphysical conditions near cloud top. Based on their results, thresholds for CRE ($>14 \mu\text{m}$), COT ($<1 \text{ K}$) and CTT ($<260\text{K}$) that were much consistent with observed rain rates has been adopted for this study.

First, the link derived rain rates are compared with CTT from MSG IR 10.8 micron channel to assess the strength of the relationship between the two observations. The modelled rain rates are further compared with CRE and COT derived from multispectral analysis of MSG IR channels 3.9, 10.8 and 12.0 respectively. This is to verify if the observed rain rates are consistent with the temporal variations in these cloud microphysical conditions. All cloud analysis were done using Integrated Land and Water Information System (ILWIS) software: versions 3.31, 3.7.2 and 3.8.5.

3.4.2.1. Parallax correction

Prior to verifying this relation the satellite derived products are first corrected for geometric effects. Parallax effect is a geometrical effect that results in apparent displacement in cloud position due to satellite viewing angle (“The Problem of Parallax,” 2006). It is more pronounced when observing high clouds or when cloud positions are far from nadir. As such, it results in mapping deficiencies—since the respective positions of clouds, with respect to the satellite, move away from their original position (Lábó et al., 2007). The zenith viewing angle of MSG varies between 39.4 and 48.5 degrees in the west and east of Kenya respectively. As such, the top of clouds are projected to the east on MSG images—resulting in a parallax offset that can amount to more than 4 pixels (Hoedjes et al., 2014; Hoffmeister et al., 2013).

As indicated by Lábó et al. (2007) the extent of parallax displacement depends on the height of the cloud tops. Hence, an estimate of the cloud top height (CTH) is a key factor in estimating parallax offset and subsequent pixel by pixel parallax correction of cloud location in satellite images.

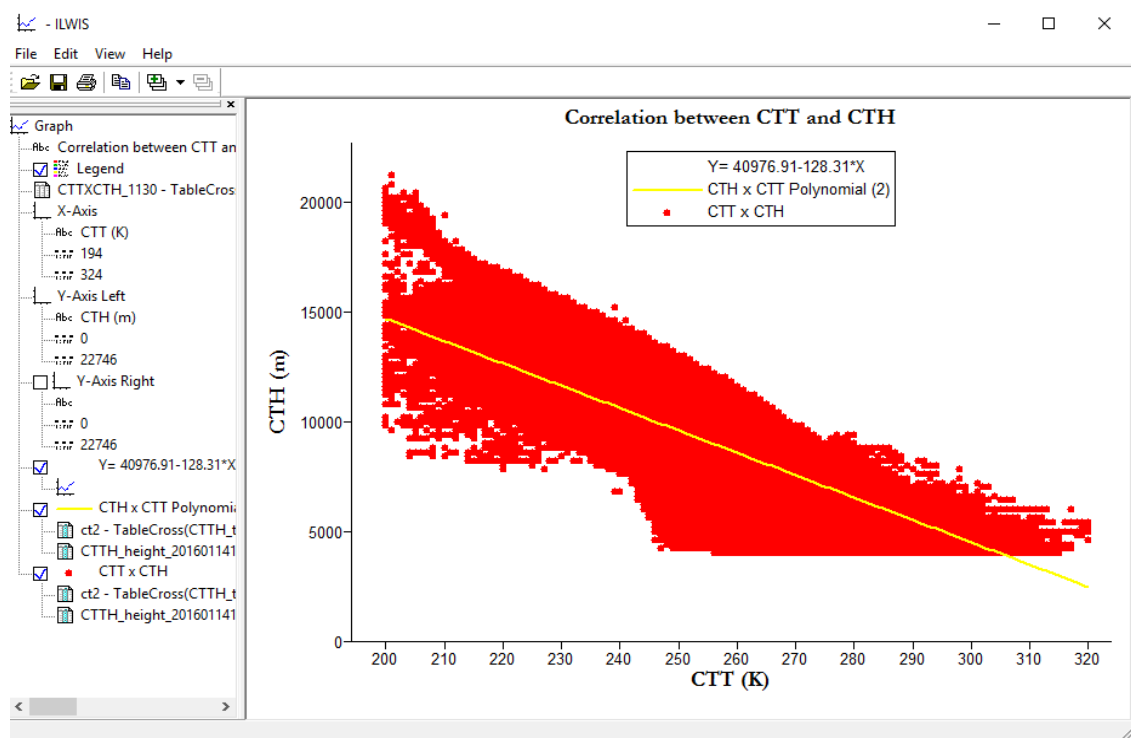


Figure 9 Correlation between CTT and CTH

For this study, obtaining CTH estimates was a challenge since archived satellite data for CTH estimates for the study period was not available. Nonetheless, an approximate estimate of CTH for the experimental period is calculated using real time data. First, a correlation was established between CTT and CTH for the period 14th January 2016, 11:30 AM as shown in Figure 9.

It can be noted there is a negative relation between CTT and CTH as would be expected. The resulting regression equation (indicated in Figure 9) is used to estimate CTH for the experimental period. All MSG images are corrected for parallax effect using this CTH estimates

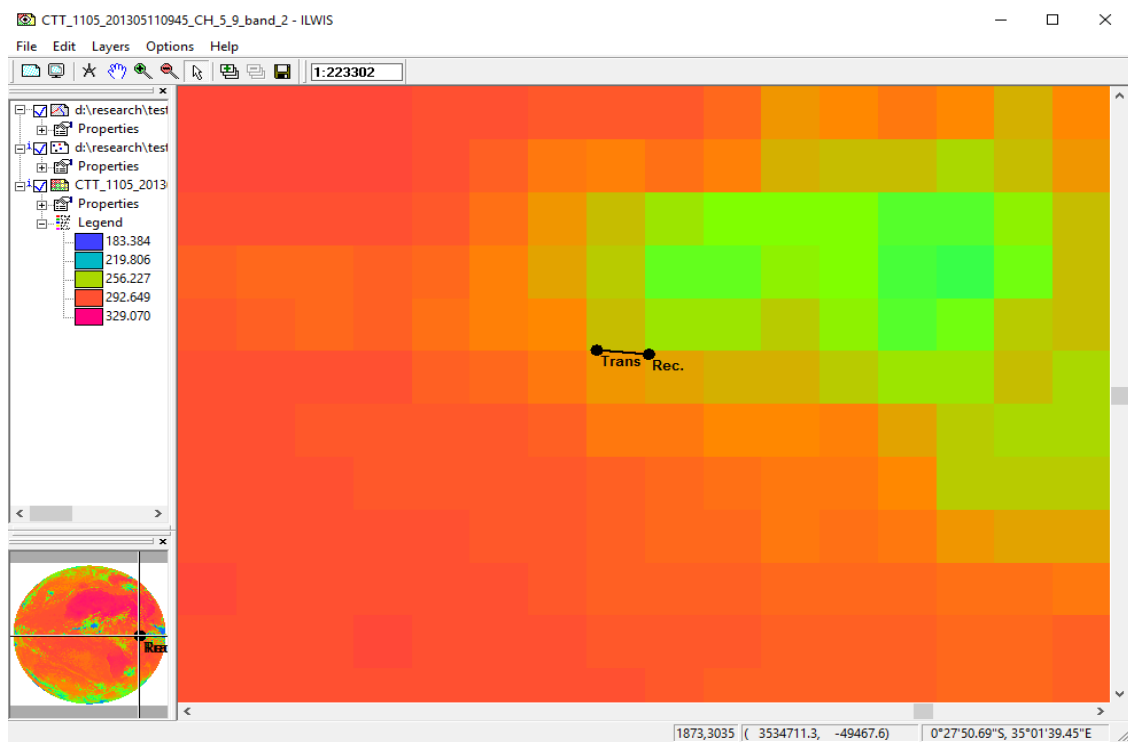


Figure 10 MSG scene not corrected for parallax effect

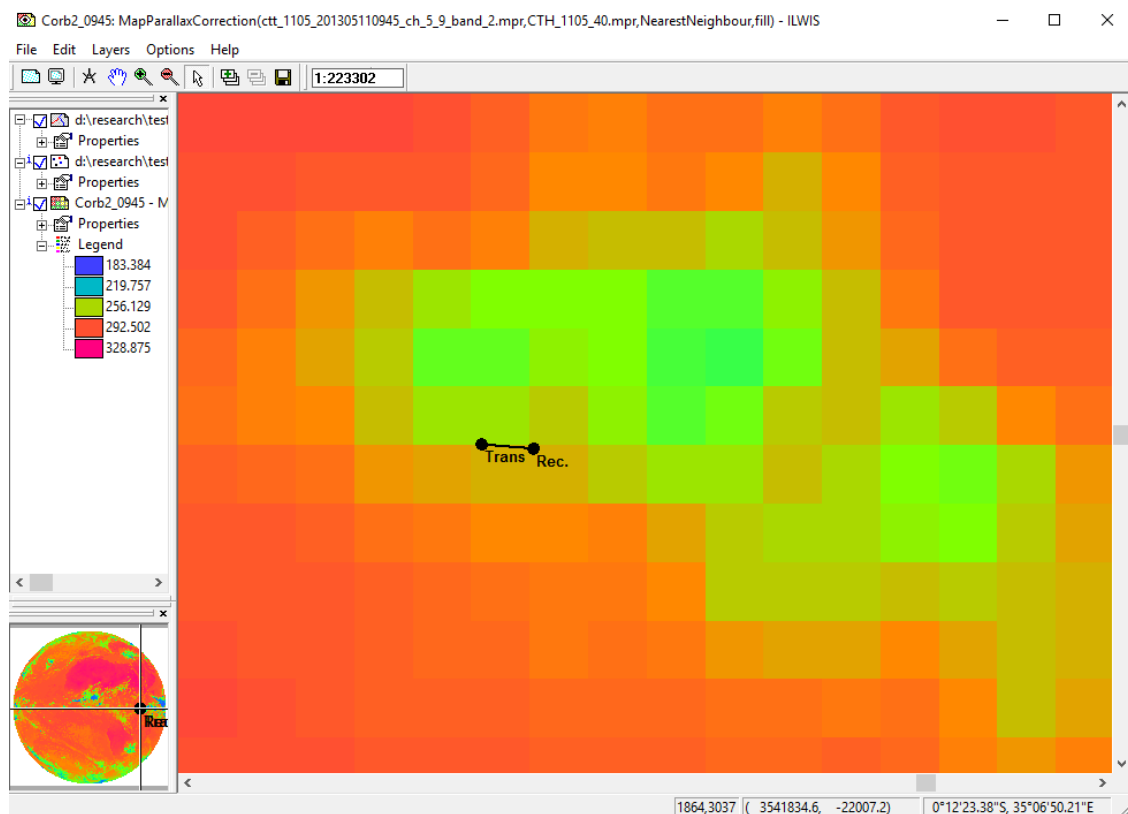


Figure 11 MSG scene corrected for parallax effect

In both images, black dots joined with black line indicates MW link transects. Trans and Rec are transmitting and receiving antenna respectively. Coloured background is MSG (IR 10.8 micron channel) scene. MSG scene indicates the CTT, which decreases from hot (red/orange coloured in image) to cold (blue coloured in image). Both images are displayed in the same zoom (1:223302)

In Figure 10 (original MSG image) and 11 (corrected MSG image), the results of parallax correction is demonstrated for the period 11th May 2013, 9:45 AM. As can be seen from the image, there is an apparent shift of the position of cold pixels from top right in Figure 10, to the centre of the image view in Figure 11. The resulting corrected MSG images have approximately 2 pixel shifts (approximately 6km) from their initial position.

3.4.2.2. Relation between MW link rain estimates and MSG CTT

After correction of parallax effect in MSG images, the relation between CTT inferred from MSG 10.8 micro channel and the MW link rainfall estimates for the period of rainfall observation by the link can be verified. First, the footprint of the link needs to be projected into MSG scenes. In this way, for each period rainfall is observed by the link, the cloud cover condition surrounding the footprint of the link can be identified.

To achieve this, the link transect was converted to a line segment. The resulting segment map was then transformed to point map. The result of the transformation is a given set of four different points along the footprint of the link transect. The resulting point map is then overlaid with each MSG image to identify the cloud condition surrounding the footprint of the link.

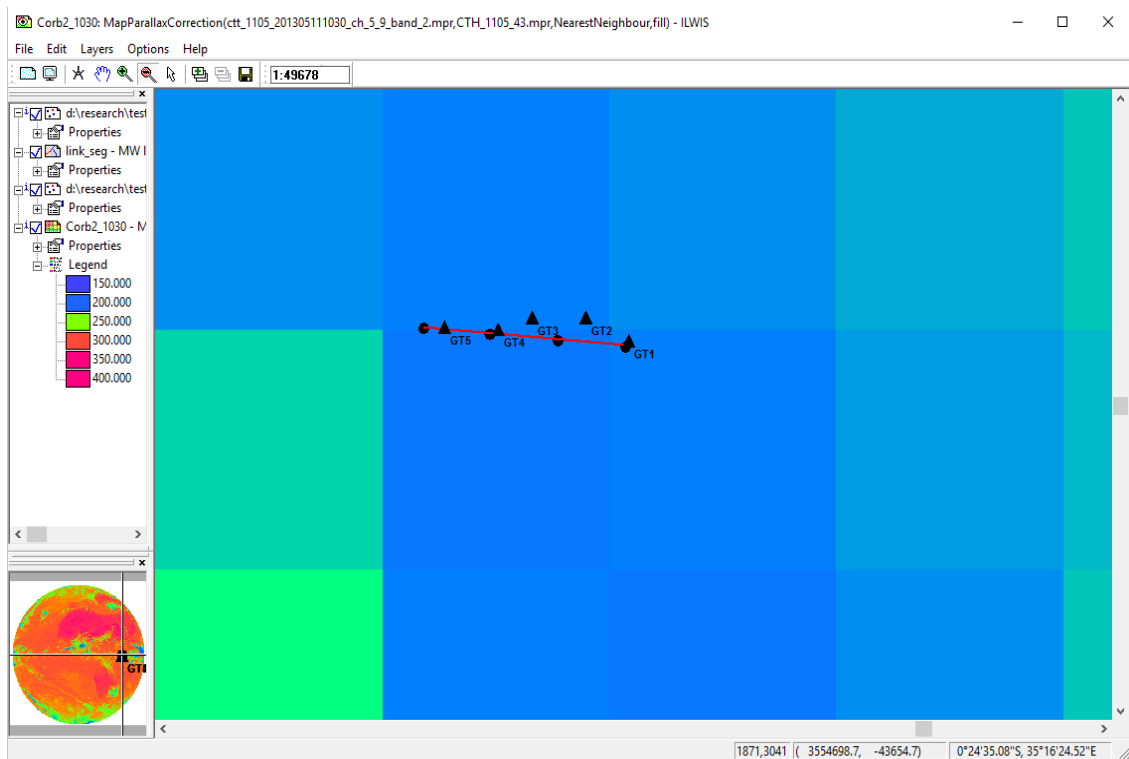


Figure 12 Microwave link transect transformed to points in an MSG scene

Black dots joined with a red line is MW link transect converted to points, black triangles are rain gauges under link transect. Coloured background is MSG (IR 10.8 micron channel) scene. MSG scene indicates the CTT, which decreases from hot (red/orange coloured in image) to cold (blue coloured in image)

Figure 12 shows MW link transect that is transformed into four points and overlaid with a parallax corrected MSG image for the period of 11th May 2013, at 10:30 AM. It can be seen that for the rain event that occurred on the said period, a large storm that passed over the area of the link covered the entire footprint of the link. Since the rainfall intensity derived from the microwave link represents a path average rain rate along the link transect (Townsend & Watson, 2011), it is assumed that all the resulting point created from the link all have the same rain rate. The idea to represent the link transect as a point in order to incorporate with other information is also demonstrated by Messer et al. (2008)

Next, the resulting point map is crossed with the respective images from MSG. Since the points on the link transects are located within the area of three pixels, an average pixel value of all the three pixels is used as the CTT for the cloud surrounding the foot print of the link. The output table from the cross operation is then used in establishing the correlation between the two.

3.4.2.3. Relation between MW link rain estimates and CRE, COT

Cloud microphysical properties CRE and COT are derived based on multispectral analysis using the approach illustrated by Rosenfeld & Gutman (1994). MSG IR channels 3.9, 10.8 and 12.0 are downloaded for the same period, 11th May 2013, as the rain event. All images downloaded were corrected for parallax shift using CTH estimates derived for the same period as the MSG image.

CRE is derived based on spectral difference between IR 3.9 and IR 10.8 microns. A threshold of $> 14 \mu\text{m}$ is used to identify cloudy pixels with high CRE and therefore have the potential to precipitate. Similarly, COT is also derived based on spectral difference between IR 10.8 and 12.0 μm . A threshold of $<1 \text{ K}$ is used to identify cloudy pixels that are optically thick and as such have high potential to precipitate. Likewise, the resulting maps from the spectral differencing are overlaid and afterwards crossed with the point map from the MW link, as illustrated in the MW link CTT relation procedure. In this way, the microphysical property of the cloud cover over the link transect at any period can be observed, whereas the value of the pixel can be retrieved from the output table from the cross operation. The pixel values for each of the cloud property are retrieved and analysed, using the aforementioned thresholds, and with respect to the link derived rain intensities for each period rain occurred.

4. EXPERIMENTAL RESULTS

4.1. Comparing MW link rainfall estimates to PAR from rain gauges under link transect

In Figure 13, the calibration results for link rainfall estimates are presented for the period 11th May 2013. Initial simulations (indicated in Figure 13 as a and b) shows significant overestimation by the algorithm compared to PAR from rain gauges under link transect. In Figure 13 (b), r^2 values for the MW link rainfall estimates based on each the 3 coefficients are low—indicating a weak agreement between the modelled rainfall intensities and the observed rain intensities. This is due to overestimation of rain intensities, especially at high rain events by the MW links based rain estimation algorithm. This is likely due to wetting of the antenna at the onset of rain and continues to affect signal transmission even after rain has ceased (Leijnse et al., 2007a, 2008; Kharadly & Ross, 2004; Zinevich et al., 2010).

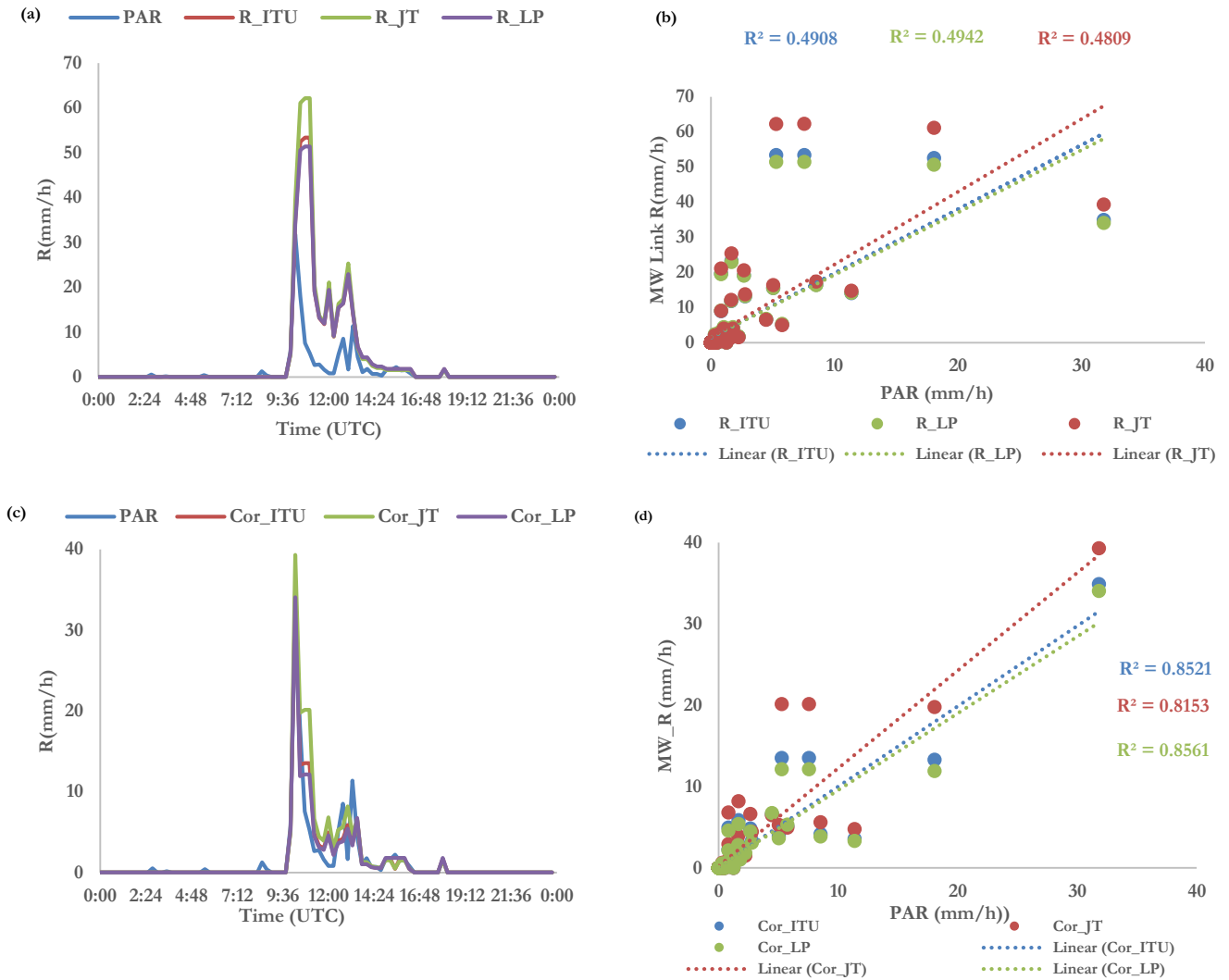


Figure 13 Calibration results for MW link rainfall retrieval
Where R_{ITU} , R_{JT} and R_{LP} in Figure b is rain rates based on ITU, JT and LP coefficients respectively, Cor_{ITU} , Cor_{JT} and Cor_{LP} is ITU, JT and LP rain rates corrected for wet antenna effect

4.1.1. Estimating wet antenna correction factor

Wet antenna is observed by coupling observations made from rain gauges installed closer to the antennas and cloud conditions retrieved from MSG images. Apparently, wetting of the antenna surfaces would occur in almost all rain events, especially after high rainfall intensities. In those observations that were considered to be probably due to wetting of the antenna, it was observed that for a high attenuation from the link, there was either a considerably low or no rainfall recorded in the rain gauge close to the antenna (see Figure 7 for signal attenuation and corresponding rain gauge estimate for 12:00 PM). Also, in most cases, the cloud microphysical properties retrieved were not consistent with the ground observation from the link (see appendix 4 for corresponding cloud microphysical properties for the same period). Such observations were considered unusual—thus the high attenuations observed were considered as probably due to wetting of antenna surfaces during previous high rain events. For this study, the complexity in the approach for estimating wet antenna, example by Kharadly & Ross (2004), is ignored due to lack of enough data. Instead, a simple wet antenna (A_w) correction factor is derived from the peak rain intensity observed by PAR from rain gauges under link transect and the peak rain intensity observed by the MW link due to wet antenna attenuation (see appendix 3 for illustration).

Coefficient	Derived A_w correction factor
ITU	0.25
JT	0.32
LP	0.23

Table 7 Estimated wet antenna correction factors for coefficients used

Table 7 indicates the different wet antenna correction factors derived based on the different coefficients used. These correction factors are applied to all incidence of overestimation by the algorithm due wet antenna attenuation.

Time	PAR	R-uncorrected (mm/h)			R-corrected (mm/h)		
UTC	mm/h	ITU	JT	LP	ITU	JT	LP
10:45 AM	7.56	53.38	62.22	51.43	13.35	19.91	11.83
11:15 AM	2.65	19.16	20.55	19.03	4.79	6.58	4.38
12:00 PM	0.82	19.61	21.08	19.46	4.90	6.75	4.48
12:15 PM	0.80	8.97	9.05	9.11	2.24	2.90	2.10
12:30 PM	5.03	15.49	16.34	15.48	3.87	5.23	3.56

Table 8 Instances of overestimation by wet antenna and correction applied

Where R-uncorrected and corrected (mm/h) is uncorrected and corrected modelled rain rates for overestimation due to wet antenna surface, PAR is path average rain rates from rain gauges under link transect

In Table 8, some instances of overestimation due to wet antenna surface and its correction are presented for the different coefficients used in retrieving rainfall from MW links. These illustrations are done based on the calibration results in Figure 13 above. It is also obvious that the link derived rain rates based on the 3 different coefficients still show some overestimation even after wet antenna correction is applied.

In Figures 13 (c and d) and the effect of wet antenna correction on link derived rain rates is demonstrated. It is apparent that the estimation and application of wet antenna correction factor was relevant; as the agreement between modelled and observed intensities from PAR from gauges under link transect is improved quite significantly. Considering the tropical rain event that was observed, the a and b coefficients reported by Olsen et al. (1978) as Joss et al. (J-T) and Laws and Parson (LP), and that of ITU (2005) all gave good estimates in comparison with PAR from rain gauges under the link transect as can be seen from Figure 15 (for c and d).

In Figure 14, the cumulative graphs for the modelled rain rates based on the three different coefficients (indicated in Table 5) and PAR from rain gauges under the link transect, are compared.

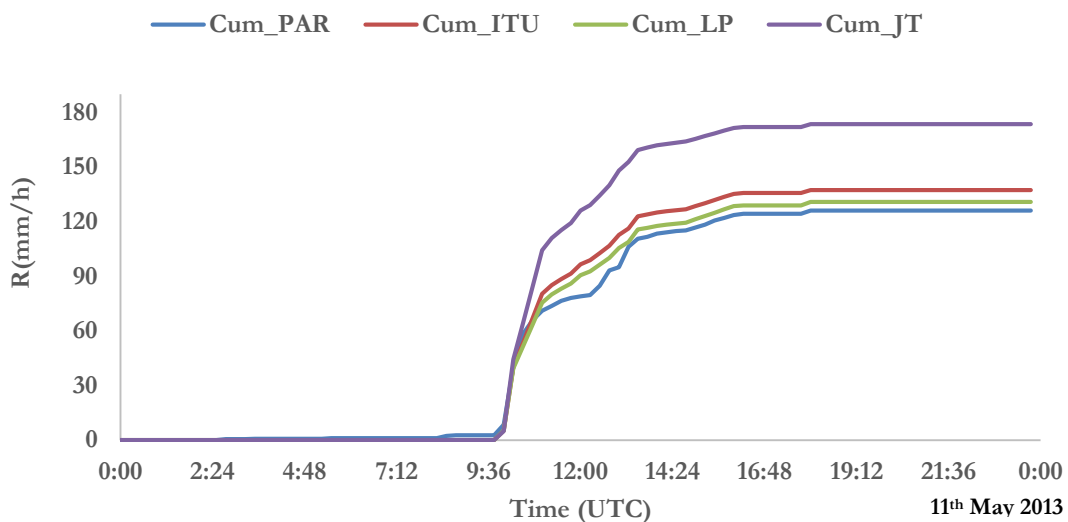


Figure 14 Comparing cumulative graph of modelled and observed rain rates Where Cum_PAR is graph based on rain from path averaged rain rates from gauges under link transect, Cum_ITU is cumulative graph based on estimates using ITU coefficients, Cum_LP is estimates based of LP coefficients and Cum_JT is cumulative graph based on estimates using JT coefficients.

The overestimation pointed out earlier on the part of JT coefficients is obvious in this illustration. The widely used LP coefficients and the ITU reported coefficients all gave fairly equal estimates with high accuracy as can be seen from Table 10.

4.2. Correlation between link rain estimates and MSG cloud microphysical properties

Figure 15 illustrates the general relation between CTT based on MSG IR 10.8 micron channel and the observed rain rate from MW link for the rain event that occurred on 11th May 2013. The general trend between the ground based rain observation from the MW link and the CTT are consistent with observations made by Rosenfeld & Gutman (1994), Vicente et al. (1998), Rientjes & Alemseged (2007). Higher rain rates generally correspond with colder cloud tops (<240 K) whereas clouds with increasing cloud top temperature produces little or no rain.

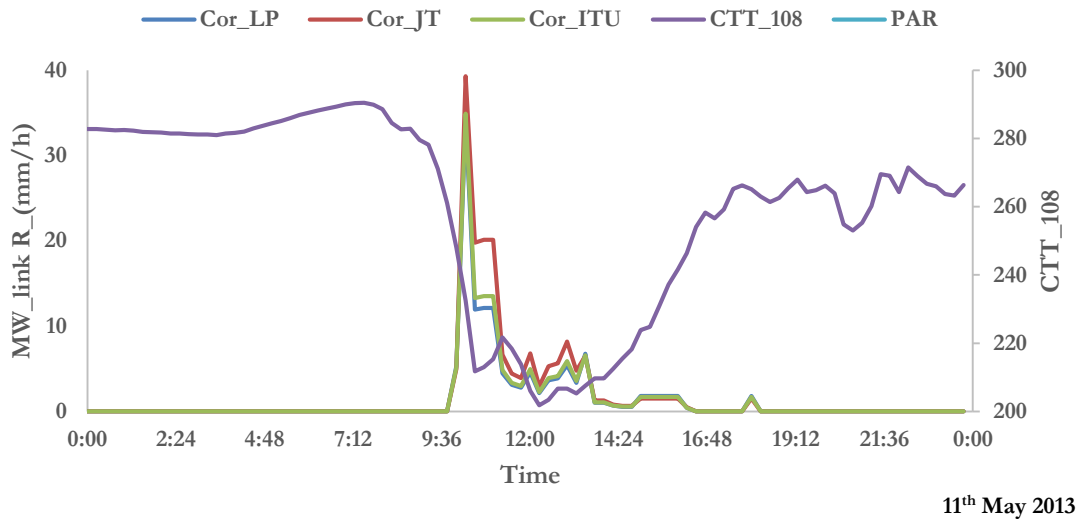


Figure 15 Relation between MW link rain estimates and MSG IR CTT using 10.8 micron channel where Cor_ITU, Cor_JT and Cor_LP denotes rain rates, derived and corrected for wet antenna attenuation, using ITU, JT and LP coefficients respectively

In Figure 16, a scatter plot of MSG IR CTT and MW link derived rain rates using 3 different coefficients in Table 3 is shown.

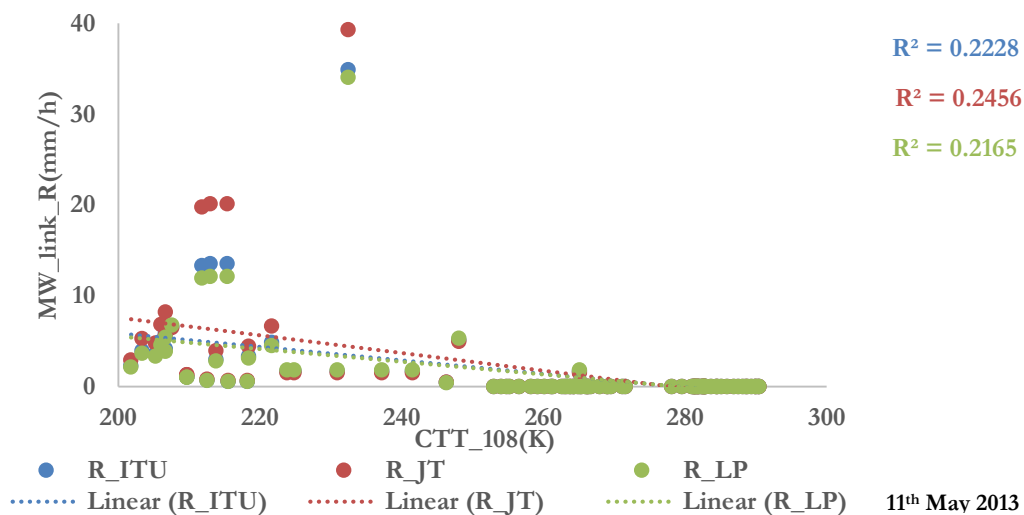


Figure 16 Scatter plot between MW link derived rain rates and CTT_10.8 micron channel

Where R_ITU, R_JT, R_LP denotes MW link derived rain rates using ITU, JT and LP coefficients respectively.

It can be observed that the r^2 for all 3 relations; R_{ITU} , R_{JT} , R_{LP} with PAR from rain gauges under link transect is significantly low, thus indicating weak relation between the two. This could probably be due to the temporal dynamics of clouds due to its life time (Rientjes & Alemseged, 2007). To improve the relation in Figure 16, the link derived rain rates are adapted to the various stages of cloud development as identified by Vicente et al. (1998) based on IR CTT variations. The evolutionary stages of cloud development identified for the experimental period includes:

- 1) initial stages of cloud development where vertical motion of clouds, due to strong updraft, is very active thus resulting in sharp decrease in CTT with height
- 2) mature stage where vertical growth is limited and as such CTT variation is comparably small but still cold
- 3) and lastly, the decaying phase of clouds where cloud tops becomes warmer with time

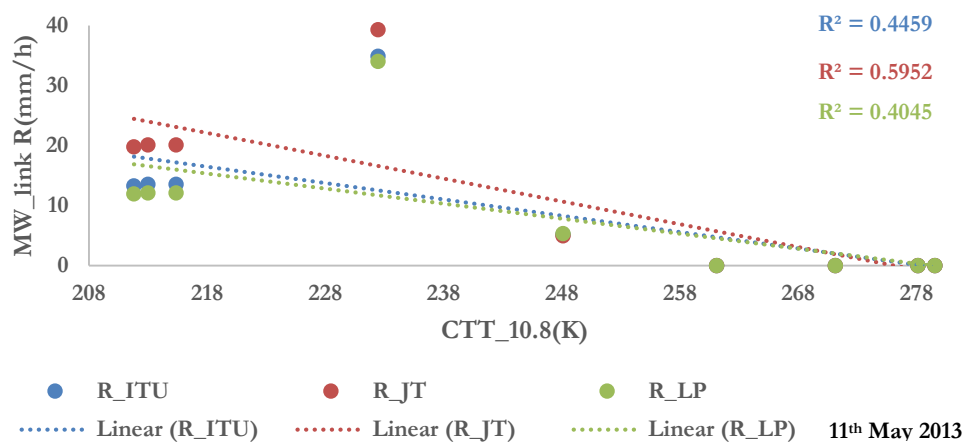


Figure 17 Comparing MW link rain rates to CTT_10.8 micron channel at the early stage of cloud development

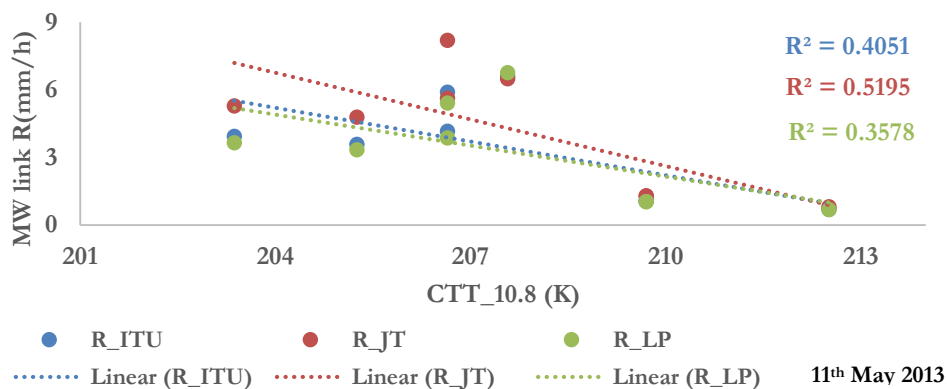


Figure 18 Comparing MW link rain rates to CTT_10.8 micron channel at the mature stage of cloud development

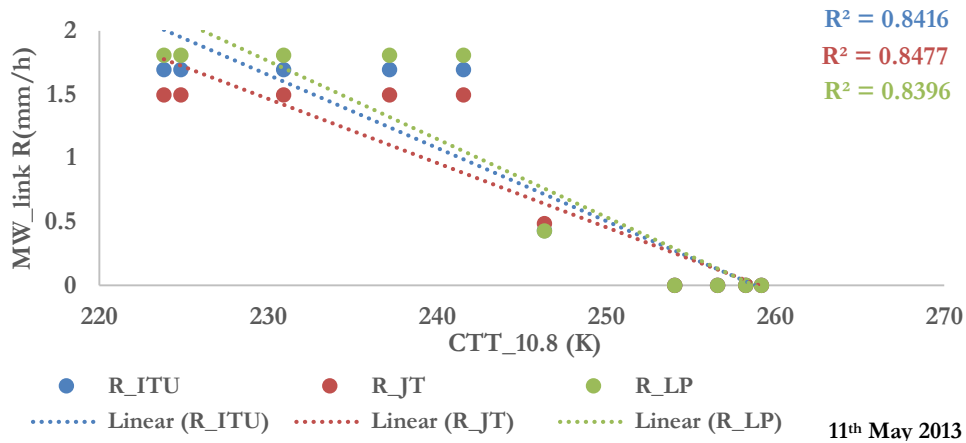


Figure 19 Comparing link derived rain rates to CTT_{10.8} micron channel at the decaying stage of cloud development
 Where R_{ITU}, R_{JT}, R_{LP} in all 3 Figures denotes MW link derived rain rates using ITU, JT and LP coefficients respectively.

In Figures 17, 18 and 19, relation between link derived rain rates and CTT for each stage of cloud development are shown. The coefficient of determination improved, but the relation between rain rates and CTTs is still not strong (especially for the initial and mature stages of cloud development) and even cold CTTs do not uniquely correspond to high rain rates. Nonetheless, decreasing CTTs still correspond to rain observations. However, these discrepancies are not different from observations made and explained by Rientjes & Alemseged (2007)

Also, the evolutionary development of cloud based on growth in CRE with decrease in temperature is analysed for the various stages aforementioned, as illustrated by (Rosenfeld, 2007). Figures 20 depicts temporal variations in CRE with changes in CTT for the various stages of cloud development identified in the cloud analysis for rain observation.

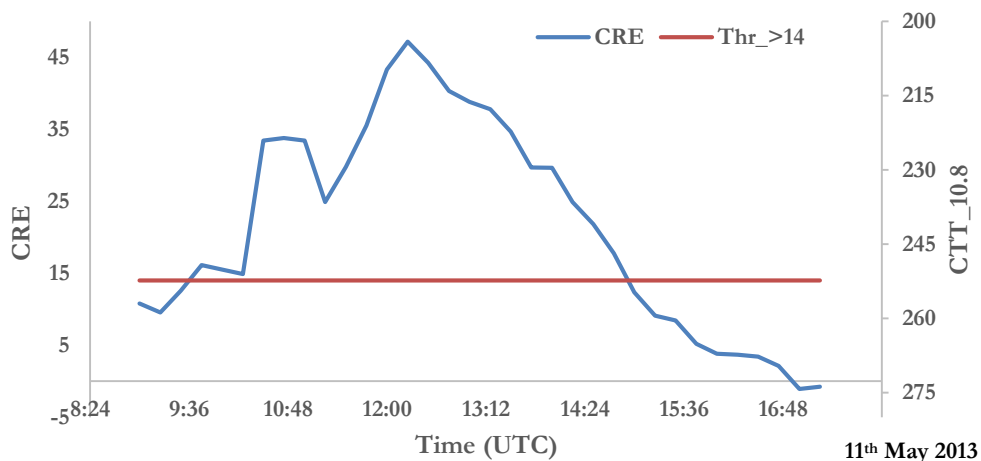


Figure 20 Temporal variation in CRE with variation in CTT
 Where CRE in first y-axis is cloud effective radius, CTT_{10.8} in second y-axis is MSG IR CTT using 10.8 micron channel and Thr_{> 14} (indicated as red line in image) is adapted threshold for inferring rain from clouds for the different periods rain was observed by the link

It can be observed that, the development of clouds, as indicated by temporal variation in CRE with CTT is consistent with guidelines adapted by Vicente et al. (1998). During the initial stages of cloud development (from 9:00 AM to 12:00 PM), there is sharp drop in the CTT due to strong updraft—which also shows build up CRE because clouds are intensifying and with phase including large droplets to large and small ice crystals. This is also consistent with high rain intensities observed for that period. Mature stage (between 12:00 PM and 14:00 PM) depicts decline in CRE, yet with cold cloud tops (consisting mainly of ice crystals), but low rain intensities—possibly due to large rain intensities during initial stage. Also there is minor change in CTT, probably because vertical motion have ceased. The decaying phase (after 14:00 PM) depicts comparatively warmer temperatures which are also consistent with low CRE derived and rain rates observed for that period. Nevertheless, discrepancies between cloud properties and observed rain rates from MW link still exists for some rain events; for instance during the mature stages, between 12 and 2:00 PM.

Also the relation between CRE and COT with respect to their respective thresholds for rainfall observation from clouds, is analysed. Figure 21 illustrates the relation between COT and CRE for cloud cover condition during the period of 11th May 2013 when rainfall is observed by the link.

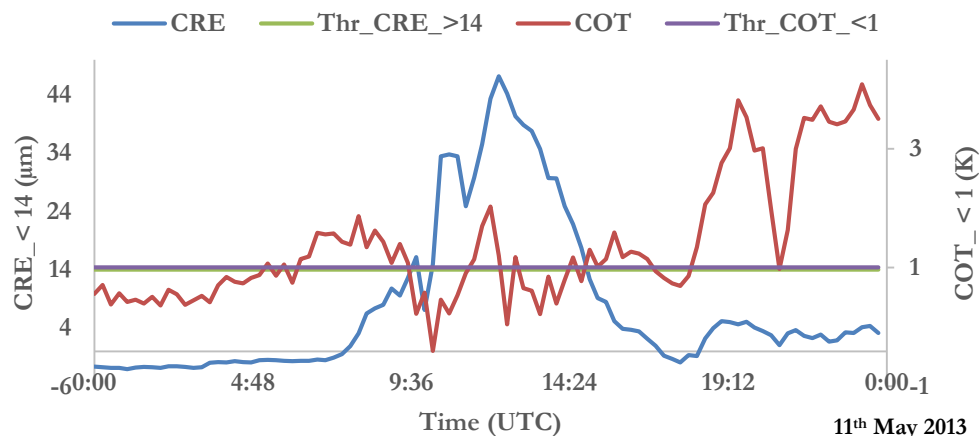


Figure 21 Relation between CRE and COT for rainfall retrieval from clouds

Where CRE_>14 is values for CRE while considering a threshold above 14µm, COT_<1 is values of COT while considering a threshold below 1K, Thr_CRE_>14 is threshold line for CRE and Thr_COT_<1 is threshold line for COT

Analysis is made based on thresholds adapted from Rosenfeld & Gutman (1994). Threshold lines for CRE and COT are both illustrated. The threshold combination presents an inverse relation between CRE and COT for inferring rainfall from clouds. For CRE, there is an increasing order ($> 14 \mu\text{m}$) of magnitude as an indicator for clouds with large effective radius; whereas COT adapts a decreasing order ($<1\text{K}$) of magnitude as an indicator for optically thick clouds. Most of the rain events captured by the MW link occurred between 9:00 AM and 14:00 PM (see Figure 13: a and c). It can be seen from Figure 21 that the inverse relation between CRE and COT is captured within the same period as illustrated in Figure 13. Hence indicating a good relation between ground based observation from the MW link and satellite derived cloud microphysical properties. This probably explains why lower rain events were observed by the link even at comparatively lower CTTs and higher CREs during mature stage of cloud development; because cloud were optically thin in most cases. Nevertheless, some discrepancies exist for some events; for instance at 12:00 PM, cloud depicts low COT ($>1\text{K}$) with high CRE, yet rainfall was observed by the link.

4.3. Combining cloud microphysical properties for detecting potential precipitating clouds

The idea is to combine the identified near cloud top microphysical properties to identify potential precipitating clouds (herein considered as convective clouds) in SEVIRI MSG images. Convective clouds are characterized by active vertical growth, low CTTs, high COTs (Henken et al., 2011; Thomas et al., 2009) and large effective radii (Young et al., 2013). Considering these characteristics, the threshold adapted from the work of Rosenfeld & Gutman (1994), for CRE and COT, and Kidder et al., (2005) for CTT is applied individually for each cloud property but then combined to determine for each pixel whether or not it qualifies to be a convective cloud. Such a technique is also demonstrated by other authors in several studies including; Henken et al. (2011), Rossow & Schiffer (1999) and Young et al. (2013).

COT (K)	CRE (μm)	dCTT (BTD 6.2 and 10.8 micron channels K)
<1	>14	< 14

Table 9 Threshold combination for detecting convectivity

Where dCTT is cloud top temperature based on brightness temperature difference between 10.8 and 6.2 micron channel

Table 9 indicates the adapted thresholds used in identifying convectivity in MSG images. Based on this threshold analysis technique, cloudy pixels within MSG scenes have to pass all threshold criteria for it to be characterized as a convective cloud. Convective clouds characterized based on this criteria is compared with link derived rain intensities to establish the relationship between the two.

In Figure 22, connectivity over MW link is demonstrated for the cloud cover on 11th May 2013, 10:15 AM. Applying the multi threshold combination results in pixel by pixel cloud characterization which generates a time series binary map, at the resolution of MSG, of clouds with or without connectivity.



Figure 22 Convectivity over MW link transect

Black dots joined with a black line is MW link transect, Trans and Rec. are transmitter and receiver respectively

Clouds in Figure 22 above, are characterized from 0 to 3. Clouds indicated as 0 (blue) means it did not meet any of the requirement of the cloud properties. Those classified as 1 (green) and 2 (orange) implies they met 1 and 2 requirements respectively whereas those classified as 3 (red) means they meet all requirements. The cloud condition as classified by the algorithm in Figure 22 is consistent with the rain intensities observed by the link for the same period (which is the highest rain observation).

4.4. Validation results

The validity of link based approach for rainfall estimation and the relation between link rainfall estimates and cloud microphysical properties is presented in this section. It is however worth knowing that, moderate to low rainfall intensities dominates the observation on this period, which are not similar to observations on 11th May 2013. As such the cloud relation algorithm might show some discrepancies with the ground observation from the link.

4.4.1. MW link rainfall estimation

The results of validating link rainfall retrieval algorithm are presented in Figure 23 below, based on rain events that occurred on 12th May 2013.

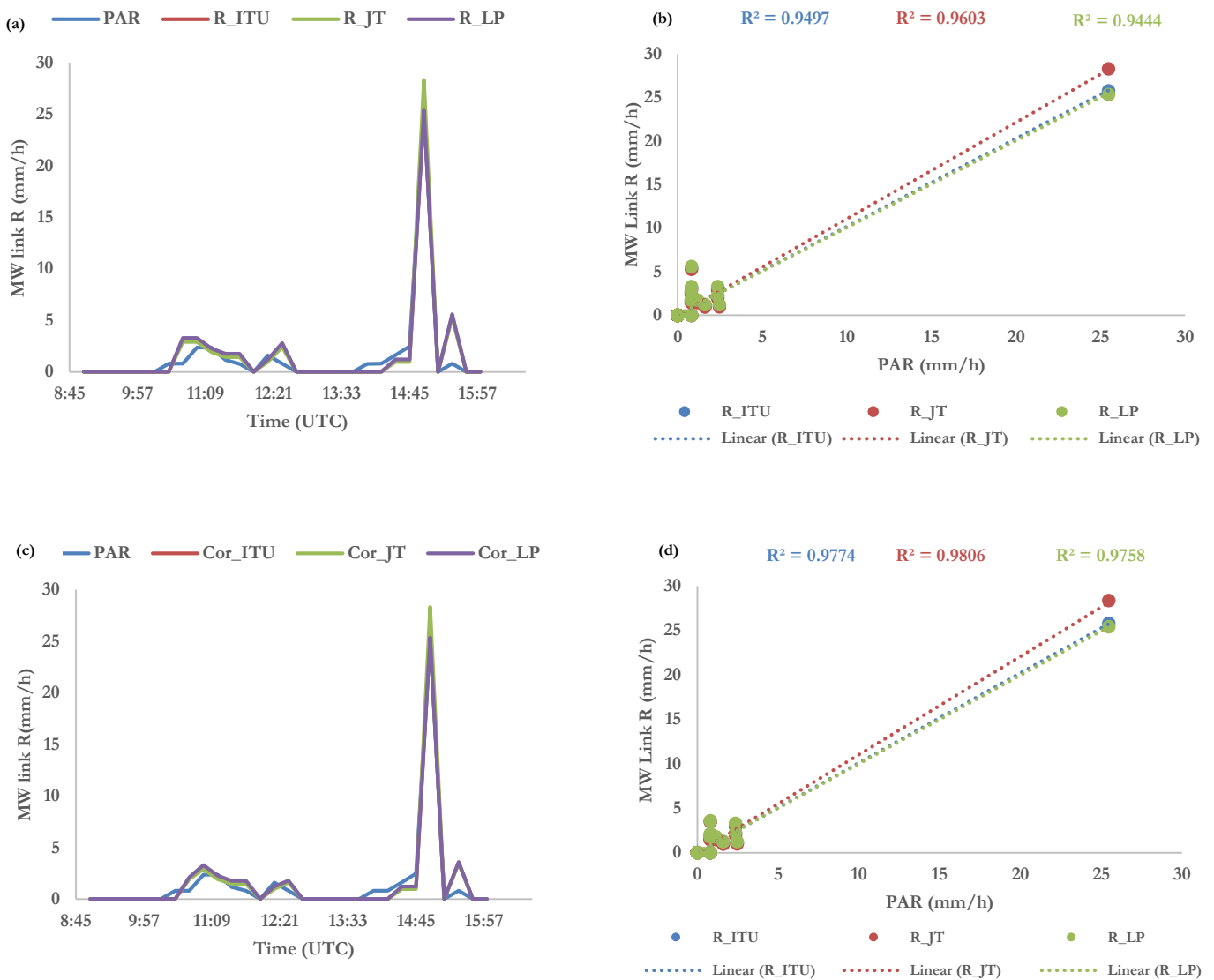


Figure 23 Validation results for MW link rainfall retrieval
Where R_ITU, R_JT and R_LP in Figure b is rain rates based on ITU, JT and LP coefficients respectively, Cor_ITU, Cor_JT and Cor_LP is ITU, JT and LP rain rates corrected for wet antenna effect

Rain events that occurred during this period are modelled based on prefactor indicated in Table 5 and using equation 2. Modelled rain events are then compared with PAR from the five gauges under the link transects. Similarly, the algorithm shows some overestimation of the observed average rain rates from the rain gauges as can be seen from Figure 23 (a and b) which again, might be due to wetting of the antenna. Also, incidence of overestimation due to wetting of antenna surfaces are corrected using the procedure aforementioned. Eventually, the agreement between modelled and observed rain rates from PAR from rain gauges under link transect is improved as can be seen from Figure 23 (c and d).

Although, the rain events that were observed on this period are comparatively low, the agreement between the modelled and the observed PAR from rain gauges under link transect is better than events observed on 11th May 2013.

4.4.2. Relation between MW link rain and cloud microphysical properties

Spectral channels for 6.2, 10.8, 3.9 and 12.0 micron channel are downloaded and parallax corrected using the procedure described earlier. As illustrated earlier, cloud top microphysical properties derived from these images are compared with modelled rain events to assess the validity of the relationship observed previously for 11th May 2013.

First MSG IR 10.8 μm CTT was derived and compared with the modelled rain events, followed by spectral differencing to retrieve CRE and COT and subsequent comparison with modelled rain events from MW link. Cloud convectivity analysis is again performed using the aforementioned threshold analysis technique to validate the relation between link derived rain rates and cloud cover condition for this period.

In Figures 24 and 25, the relation between MW link derived rain rates and cloud top microphysical properties; IR 10.8 μm CTT, CRE and COT is shown respectively.

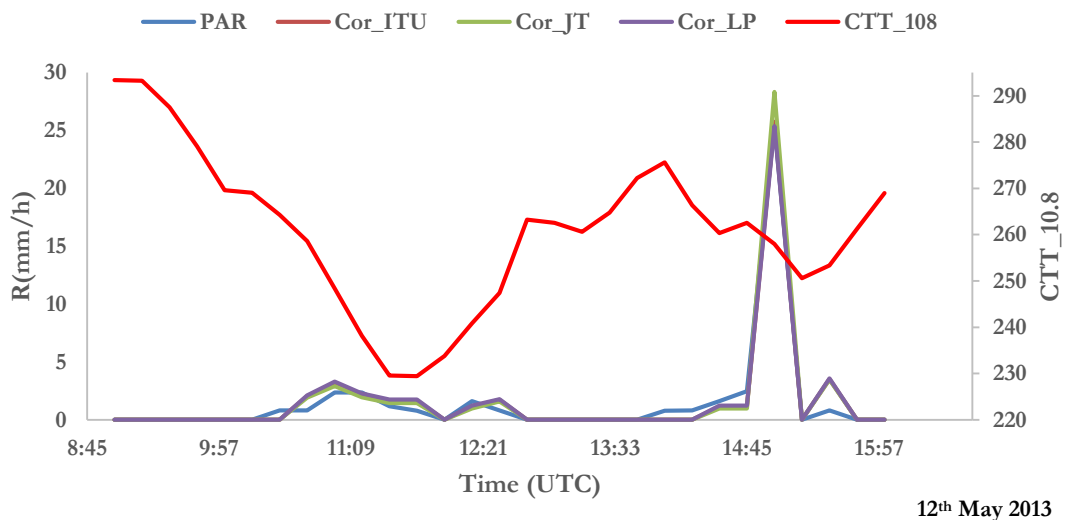
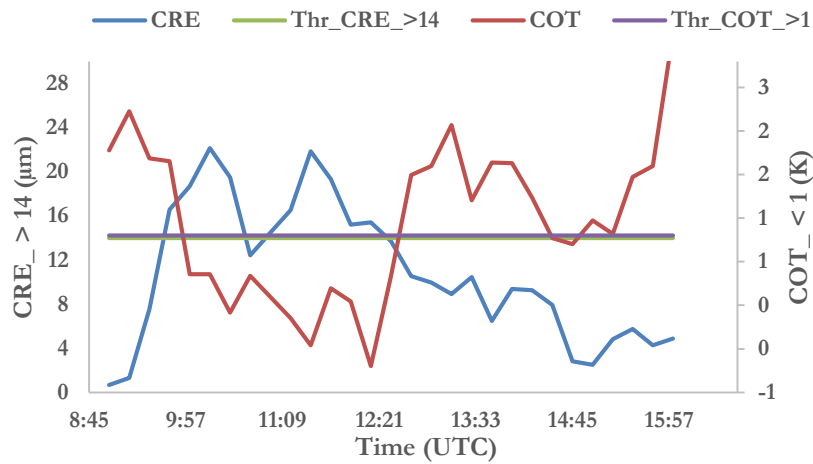


Figure 24 Relation between MW link rain estimates and IR CTT using 10.8 micron channel



12th May 2013

Figure 25 Relation between CRE and COT

Generally, the relation between MW link rain estimates and near cloud top microphysical properties is weak. In Figure 24, the relation between link derived rain rate and CTT is assessed. It can be observed that, although the general inverse trend between CTT and link based rain rates in Figure 15 repeats itself, the relationship in terms of corresponding rainfall intensities that was observed is weak. This might be due to the fact that, the rain event that was observed in this period is not typical of convective systems and so the robust relationship between CTT and observed rain intensities identified in 11th May relation, tends to weaken. As such showing much discrepancies between cold cloud tops and rainfall intensities.

Similarly, the weak relationship is reflected in the CRE COT relation in Figure 25 for assessing the relation with link derived rain rates. Although the relation is consistent with events that occurred between 10:00 AM and 13:00 PM, much discrepancies exist between the observed rain intensities—and even, it fails to capture rain events that occurred later on between 14:00 PM and 16:00 PM.

Analysis of the thermal profile for this period (see appendix 5b) reveals that, most of the clouds that caused most of the rain events on 12th May 2013 were comparatively of low altitude, with temperatures ranging between 260 and 230 Kelvin. Such clouds are not of convective systems (possibly stratiform clouds) and as such might explain why low to moderate rain intensities were observed, as well as the large discrepancies between cloud cover condition and ground observation from MW link.

4.5. Error analysis

The performance of MW link rainfall retrieval algorithm and its validation based on all 3 coefficients as well as their comparison with observed rain rates from PAR and cloud cover conditions is statistically evaluated. Statistical analysis is done by comparing link derived rain estimates to PAR from rain gauges under link transect, and to cloud convectivity analysis based on bias, coefficient of determination (r^2), coefficient of correlation (r), probability of detection (POD), number of hit signals (H), number of missed signals (M) and number of false signals (F). The estimates for POD is calculated as illustrated by (Roebeling & Holleman, 2009) based on equation 3.

Equation 3 Estimating POD

$$POD = \frac{H}{H+M} \quad (3)$$

Between PAR and link rain intensities, a rain event is considered a hit if rain gauges records an event and the link also observes the rain event. Conversely, if rain gauges observes a rain event and the link does not then it is considered a missed rain event.

Also, between the modelled rain intensities and cloud convectivity analysis (indicated in Tables 10 and 11 as CC.), a signal is considered a hit if the satellite derived products classifies a cloud as a potential precipitating cloud and the link also observes a rainfall event for the same period.

However, if the link observes a rain event and the satellite fails in classifying the cloud cover as a potentially precipitating cloud, then it is considered a missed signal. A false signal is when the satellite product classifies the cloud as potentially precipitating but the link does not observe precipitation for that period. All detection and error analysis are done with respect to the occurrence of rainfall.

OBSERVATION	NO. EVENTS	TOTAL R (MM)	AVERAGE R (MM)	H	M	F	R	R ²	POD (%)	BIAS (MM)
PAR	32	126.04	3.94							
R_ITU	27	137.44	5.09	27	5	NA	0.92	0.85	84.40	0.09
R_LP	27	130.79	4.84	27	5	NA	0.93	0.86	84.40	0.04
R_JT	27	173.54	6.43	27	5	NA	0.9	0.81	84.40	0.38
CC	17	NA	NA	17	10	1	NA	NA	63.00	NA

Table 10 Statistical analysis of MW link rainfall retrieval and cloud verification results for 11th May 2013

Where H, M and F are hits, missed and false signals respectively. NA is not available. CC is cloud convectivity, M is missed signal and R (MM) is rainfall in millimetres.

Table 10 presents the calibration results of link rainfall retrieval and comparison with cloud cover condition for the period rain was observed by the link. The number of events indicated is the number of path average rain rates and transect average rain rates for the various events that occurred within the periods of 9:00 AM and 15:00 PM, on 11th May 2013. It can be observed that, the strength of link rainfall retrieval technique in detecting (as indicated by POD values) and quantifying (as indicated by average and total rainfall) rain events and estimates is very promising. Out of 32 rain events that was observed by rain gauges, 27 of them were captured by the MW link (although discrepancies between observed rain intensities exists). The 5 events that were missed by the link might be a demonstration of the drawback of the link rain estimation technique or the links inability to detect extremely low rain intensities. In principle, the link derived estimates based on all three coefficients show good agreement (correlation coefficient r , above 0.9 and coefficient of determination r^2 , above 0.8) with path averaged rain from gauges under link transect and with no false signal. High bias for JT estimates is due to its frequent overestimation especially at high intensities (as shown in Figures 15c and 23c), which is also evident in its average and total rainfall estimates in Table 8.

The performance of the convectivity analysis based on cloud microphysical properties is also quite satisfactory. Out of 27 events that were observed by the link, more than half (as indicated by the POD value) were also detected by the algorithm and in most cases with high consistency with rainfall intensities observed by the link. For instance, high rain intensity observed by the link on 10:15 (see Figure 13c) is also captured in the cloud convectivity analysis for the same period as indicated in Figure 22. Ten events were however missed by the cloud analysis—implying the cloud analysis failed in classifying such clouds as precipitating clouds. A single false event was recorded, which imply the satellite classified the cloud cover as potentially precipitating but no ground observation was made by the link.

OBSERVATION	NO. EVENTS	TOT. R(MM)	AVE. R (MM)	H	M	F	R	R²	POD (%)	BIAS (MM)
PAR	14	42.69	3.05		NA					
R_ITU	11	45.05	4.10	11	3	NA	0.98	0.97	78.57	0.06
R_LP	11	45.62	4.15	11	3	NA	0.98	0.94	78.57	0.07
R_JT	11	45.94	4.18	11	3	NA	0.97	0.96	78.57	0.08
CC	6	NA	NA	6	5	1	NA	NA	54.55	NA

Table 11 Statistical analysis of MW link rainfall and cloud validation results for 12th May 2013

Where H, M and F are hits, missed and false signals respectively. NA is not available. CC is cloud convectivity, M is missed signal and R (MM) is rainfall in millimetres.

In Table 11, the validation results are presented based on observation that occurred within the period of 10:00 AM and 14:00 PM, on 12th May 2013. The results further confirms the potential of the link based approach in rainfall estimation. As can be seen from Table 11, the performance of the link rainfall retrieval algorithm has improved. Modelled total rain intensities (mm) and averages (mm), as well bias and r^2 values for all the 3 different coefficients are consistent with observed averages from rain gauges. Out of 14 rain events, 11 were observed by the link while missing 3 events. Again, missed events by the link rainfall retrieval algorithm could be attributed to the drawback of the algorithm: link inability to estimate low rain intensities and, rainfall must occur on the link before its detected. Although, the POD is comparatively less than before, r , r^2 and biases demonstrate the significant strength of the retrieval algorithm.

Also, the strength of the convective cloud analysis, although weakened, is not very poor as can be seen from POD. This could be probably due to different rainfall type (possibly stratiform rain) that was observed for this period. As such the adapted threshold combination tends to fail, in most cases, in classifying clouds for possibility of rain.

5. DISCUSSION

An algorithm to estimate rain rate, using 3 different coefficients, based on MW link signal attenuation is explored in this study. Relation between estimated rainfall intensities and conditions of cloud cover that possibly caused the ground based observations from the MW link is also assessed. The information from the MW link are received at the same temporal resolution as the satellite information on the cloud cover, thus making it easier and feasible to infer the relation between the two.

5.1. Rainfall retrieval algorithm based on MW link attenuation

The quality of link based approach in estimating rainfall is studied by deriving rain rates using attenuation from a single 15GHz MW link and comparing with average rain intensities from 5 rain gauges installed under the link transect. The retrieval approach adapts the power law relation between attenuation information from the link and rainfall, whereas the averaged rain intensities from 5 rain gauges under link transect is computed based on the approach illustrated by Leijnse et al. (2007a). Since this is based on proximity analysis, it might not capture the high variability in rain observations in the area of study. Nevertheless, the performance of the rainfall retrieval algorithm as indicated by its POD, r and r^2 is reasonably consistent with earlier results presented by Domounia et al. (2014) for similar rainfall type in Africa. Results of first simulations as indicated in Figure 13: a and b (for calibration), and to some extent, 23: a and b (for validation) showed weak correlation with path average rain rates from five rain gauges that were installed under the link transect. This was considered to be probably due to wetting of antenna surface, as has also been reported by several authors for similar studies. By coupling rain estimates from gauges close to antenna and MSG based cloud microphysical properties, some unusual attenuation from the link were assumed to be instances of wet antenna surface (see Figure 7 and appendix 4 for 11th May 2013 illustration). A simple wet antenna attenuation factor is estimated from peak rain rates observed by PAR from rain gauges under link transect and peak rain rates observed by MW link and applied to the modelled rain rates. Although this is pragmatic approach to deal with the effect of wet antenna attenuation, the results shows the correction factors proved useful since the agreement between the modelled and the path averaged observed rain rates increased quite significantly.

Yet, the link based rain estimates using different coefficient still show some overestimation as shown in Tables 8 (for R-corrected) and Figure 13c. This, however, is not different from observations made by Rincon & Lang (2002). Although some studies (Leijnse et al., 2007a; Olsen et al., 1978) have indicated the less sensitivity of DSD to the power law relationship (notably for frequencies above 10GHz) in equation 2, the relationship has been shown to be considerably affected by variation in DSD (Rincon & Lang, 2002; Townsend & Watson, 2011). As such variation in DSD could explain

the oversimulation observed even after wet antenna correction. Also, the differences could be attributed to the nature of comparison between the two different approach of rain estimation: thus point average from rain gauge and line average from MW link. As such, the different advantages and limitations of the two approaches could be demonstrated by the algorithm. A typical situation like this occurred in both the initial simulation and validation period of the algorithm; where the link missed 8 events: 5 for 11th May 2013 observation and 3 for 12 May observation, which were captured by the gauges. The fact that MW links miss a rain event is a demonstration of its inability to detect extremely low rainfall intensities. This is because at such finer attenuations, it becomes difficult separating attenuation baseline from attenuation due to rain. Hence, some of the discrepancies in totals and averages of rainfall intensities for modelled and gauge observed estimates could be explained by this observation.

Nevertheless, the validation results indicate further improvement in the MW link rainfall retrieval for rain events observed on 12th May 2013 as can be seen from r , r^2 and bias values in Table 11 for all 3 sets of coefficients indicated in Table 5. This could be probably due to the comparatively low to moderate rain events (possibly stratiform rain) that was observed for and modelled for that period. The much better agreement observed for such events is however consistent with observations made by Rincon & Lang (2002), who also reported similar results for stratiform rain.

Overall, the respective r and r^2 values in Tables 10 and 11, reflecting on the strength of the comparison between each of the modeled rain rates (using coefficients in Table 3) and PAR from gauges under link transect, further confirms the potential of MW link based approach in rain estimation. Although, LP coefficients reported are derived from drop size distribution from continental temperate rainfall, Olsen et al. (1978) also indicated they have some validity for convective rain. Likewise, JT coefficients also apply to convective rain. The ITU-R reported coefficients, although not meant for specific predefined rainfall types but are based on specific attenuation from rain rates in mm/h; still give good estimates of rain intensities. With regards to the quality of the rain estimates using the adapted coefficients, the results presented hereafter indicates that the coefficients used are typical of the rainfall type being modeled.

5.2. Relation between MW link rain estimates and MSG derived cloud microphysical properties

Considering the apparent relation between cloud microphysical properties and precipitation (Cattani et al., 2009), the relation between the ground based observation from the MW link and the cloud cover condition was not different. Prior to computing this relation, parallax correction of MSG images was done using a CTH estimate derived from the relation between CTT and CTH in real time. Although this is error prone, in the absence of sufficient data, this seemed to be a better option.

Footprints of MW link transects are then projected into MSG scenes, such that cloud cover conditions for each incidence of rainfall could be assessed. The basic idea behind this procedure is that, for every period the link observed a rain event, a storm might have passed over the area surrounding the link. This was the basis for inferring the relation between the ground based rain rates from the MW link and convective clouds classified based on multispectral analysis of MSG IR channels for near cloud top microphysics properties.

Initial verification results (using observation from 11th May 2013) have shown that, the relation between modelled rain rates and CTTs, although good, was not strong enough—as has also been observed by other researchers. When incorporating other cloud properties: CRE and COT, some discrepancies in the relation could be explained. These observations are similar to results presented by Roebeling & Holleman (2009) who discussed in their analysis that combining information of different cloud properties led to 10% increase in explained variance and reduction in false alarms.

Quite apart from these observations, the validation results (using observations from 12th May 2013) showed relatively weaker relation. Eventhough the inverse relation between CTT and ground based rain rate from the link repeated itself, the relation was much weaker than before; and was also evident in CRE and COT relation for rain observation. Comparing thermal profiles for cloud cover on the link for two periods: 11th and 12th May 2013 (Appendix 5) indicates that clouds that possibly caused the observed rain rates were of low altitude, possibly stratiform clouds. This might explain the low to moderate rain intensities observed by the link and also the large discrepancies between the link observation and cloud analysis made from the retrieved microphysical properties. As was explained by Rientjes & Alemseged (2007), different clouds behave differently in pattern and rainfall intensities, and as such need to be parameterized differently.

Convective cloud analysis combines all three information (CTT, CRE and COT) on cloud composition to detect potential precipitating clouds (herein indicated as convective clouds). The detection involves assigning thresholds (adapted from literature) to each of these cloud properties, as has also been illustrated by other authors in similar studies. Initial performance of the algorithm according to Table 10 is quite promising; over 60% detection rate with a single false alarm. Although this performance tends to deteriorate according to the validation results in Table 11, this observation

could be attributed to the differences in rainfall phenomena that was observed for the different periods.

Overall, the complexity of rain observation from space due to cloud and rainfall dynamics that happen at different spatial and temporal dimensions limits the ability of space borne sensors to capture pertinent information with respect to rainfall (Rientjes & Alemseged, 2007). As such the marginal performance of the convective cloud analysis in relation to link based rainfall observation is not trivial.

6. CONCLUSION AND RECOMMENDATION

6.1. Conclusion

The potential of commercial MW links to give good estimates of rain intensities has already been demonstrated in the past. The intention was to use this technique in retrieving rain rates from MW links, verify and validate their relation with cloud cover conditions so that the modelled estimates could be regionalised for other areas close to the link. Due to challenges pertaining to data acquisition and locations for setting up gauges, this overall objective could not be met. However, part of the objective; which involves modelling rain rates using MW link signal attenuation and assessing relation with cloud cover is explored and its results and discussion presented in this report. Rain rates are retrieved (using 3 different coefficients) from signal loss from microwave links; and its relation with cloud cover condition based on microphysical cloud properties is investigated. As pointed out in the past, the power law relation between MW link signal attenuation and rainfall, overestimates the observed rain intensities from gauges. Nonetheless, the results based on probability of detection, the correlation coefficient r , and coefficient of determination r^2 in Tables 10 and 11 show that power law relationship still hold well for variable rain rates. Improved performance of the retrieval algorithm according to the validation results in Table 11 is attributed to the difference in rain type that was observed and modelled for that period. In principle, all 3 coefficients in Table 5 give good estimates of rain rates when compared to PAR from rain gauges under link transect, but due to the numerous applications of rainfall estimates especially in flood management, high accuracy in rainfall estimation cannot be ignored. Hence, the widely used LP coefficients and ITU coefficients would be suggested for link rainfall retrieval in this region since they both give fairly equal estimates with comparatively smaller biases.

Part of the objective was to assess the relation between the observed rain rates from MW link and cloud cover condition. As such, clouds are observed for convectivity, based on retrieved microphysical properties, and used in detecting potential precipitating clouds for the periods rain was observed by the link. Considering the results presented, the relation between observed rain rates from MW link and cloud convectivity analysed seems very much satisfactory. Although, validation results showed weaker response, this is attributed to different cloud type and as such rain observation that occurred for the different periods. Nonetheless, the overall performance of the cloud microphysical algorithm in relation to rain observation from the link is much promising.

6.2. Recommendation

The fact that the MW link information from links in this region are obtained at temporal resolution of MSG, makes both a promising tool for rainfall monitoring for this region. In future, the identified relation between link derived rain rate and cloud condition from MSG satellite data, can be further tested over a large area in near real time. Also, an algorithm can be developed, based on this relation, to regionalize the rain rate from MW link in near real time. This can also lead to MW link MSG based rainfall observation system for gauge scarce regions in Africa, since the two systems are already existing and operational but for different purposes.

In view of this, the following could be considered in future to strengthen the relation for a better rainfall monitoring;

- 1) better quantification of uncertainties in the link rainfall retrieval algorithm based on wet and dry classification of link signals, estimating reference signals etc.;
- 2) a more robust approach in setting up gauges under links and estimating path average rain rate from rain gauges;
- 3) a more accurate estimation of attenuation due to wet antenna;
- 4) characterization of rain bearing clouds with respect to cloud type, microphysical properties and rainfall process as observed by the link.

REFERENCES

- Abrajano, G. D., & Okada, M. (2012). Determining rain location through microwave mesh network signal attenuation. In *IEEE Region 10 Annual International Conference, Proceedings/TENCON* (pp. 1 – 6). Ikoma,Nara. doi:10.1109/TENCON.2012.6412326
- Atlas, D., & Ulbrich, C. W. (1977). Path- and Area-Integrated Rainfall Measurement by Microwave Attenuation in the 1-3 cm Band. *Journal of Applied Meteorology*, *16*(12), 1322–1331. doi:10.1175/1520-0450(1977)016<1322:paairm>2.0.co;2
- Cattani, E., Torricella, F., Laviola, S., & Levizzani, V. (2009). On the statistical relationship between cloud optical and microphysical characteristics and rainfall intensity for convective storms over the Mediterranean. *Natural Hazards and Earth System Science*, *9*(6), 2135–2142. doi:10.5194/nhess-9-2135-2009
- David, N., Alpert, P., & Messer, H. (2013). The potential of cellular network infrastructures for sudden rainfall monitoring in dry climate regions. *Atmospheric Research*, *131*, 13–21. doi:10.1016/j.atmosres.2013.01.004
- Domounia, A., Gosset, M., Cazenave, F., Kacou, M., & Zougmore, F. (2014). Rainfall monitoring based on microwave links from cellular telecommunication networks: First results from a West African test bed. *Geophysical Research Letters*, *41*(16), 6015–6021. doi:10.1002/2014GL060724
- Gaona, M. (2012). *Rainfall field estimation using simulated microwave link information*. Utrecht University. Retrieved October 18, 2015, from <http://igitur-archive.library.uu.nl/student-theses/2012-0116-200717>
- Gaona, M. F. R., Overeem, A., Leijnse, H., & Uijlenhoet, R. (2015). Sources Of Uncertainty In Rainfall Maps From Cellular Communication Networks. *Hydrology and Earth System Sciences Discussions*, *12*(3), 3289–3317. doi:10.5194/hessd-12-3289-2015
- Giuli, D., Toccafondi, A., Gentili, G. B., & Freni, A. (1991). Tomographic Reconstruction of Rainfall Fields through Microwave Attenuation Measurements. *Journal of Applied Meteorology*, *30*(9), 1323–1340. doi:http://dx.doi.org/10.1175/1520-0450(1991)030<1323:TRORFT>2.0.CO;2
- Hanna, J. W., Schultz, D. M., & Irving, A. R. (2008). Cloud-top temperatures for precipitating winter clouds. *Journal of Applied Meteorology and Climatology*, *47*(1), 351–359. doi:10.1175/2007JAMC1549.1
- Henken, C. C., Schmeits, M. J., Deneke, H., & Roebeling, R. (2011). Using MSG-SEVIRI cloud physical properties and weather radar observations for the detection of Cb/TCu clouds. *Journal of Applied Meteorology and Climatology*, *50*(7), 1587–1600. doi:10.1175/2011JAMC2601.1

- Hoedjes, J., Kooiman, A., Maathuis, B., Said, M., Becht, R., Limo, A., Mumo, M., Nduhiu-Mathenge, J., Shaka, A., & Su, B. (2014). A Conceptual Flash Flood Early Warning System for Africa, Based on Terrestrial Microwave Links and Flash Flood Guidance. *ISPRS International Journal of Geo-Information*, 3(2), 584–598. doi:10.3390/ijgi3020584
- Hoffmeister, D., Zellmann, S., Pastoors, A., Kehl, M., Cantalejo, P., Ramos, J., Weniger, G.C., & Bareth, G. (2013). The investigation of the Ardales Cave, Spain - 3D documentation, topographic analyses, and lighting simulations based on terrestrial laser scanning. *Remote Sensing*, 5, 1–14. doi:10.3390/rs50x000x
- Hogg, D. C. (1968). Millimeter-Wave Communication through the Atmosphere. *Science*, 159(3810), 39–46. doi:10.1126/science.159.3810.39
- ITU-R. (2005). *RECOMMENDATION ITU-R P.838-2 Specific attenuation model for rain for use in prediction methods*. Geneva, Switzerland. Retrieved from <https://www.itu.int/rec/R-REC-P.838-3-200503-I/en>
- Kestwal, M. C., Joshi, S., & Garia, L. S. (2014). Prediction of Rain Attenuation and Impact of Rain in Wave Propagation at Microwave Frequency for Tropical Region (Uttarakhand , India). *International Journal of Microwave Science and Technology*, 2014, 6. doi:<http://dx.doi.org/10.1155/2014/958498>
- Kharadly, M. M. Z., & Ross, R. (2004). Effect of Wet Antenna Attenuation on Propagation Data Statistics. *IEEE TRANSACTIONS ON ANTENNAS AND PROPAGATION*, 49(8), 1183–1191. doi:10.1109/8.943313
- Kidder, S. Q., Kankiewicz, J. A., & Eis, K. E. (2005). *Meteosat Second Generation Cloud Algorithms for Use at AFWA*. BACIMO 2005, Monterey, CA
- Lábó, E., Kerényi, J., & Putsay, M. (2007). The parallax correction of MSG images on the basis of the SAFNWC cloud top height product. In *EUMETSAT meteorological satellite conference* (p. 141 pages). Darmstadt. Retrieved July 25, 2015, from <https://www.tib.eu/de/suchen/id/BLCP:CN068094005/The-parallax-correction-of-MSG-images-on-the-basis/>
- Leijnse, H. (2007). *Hydrometeorological Application Of Microwave Links: Measurement Of Evaporation And Precipitation*. *Water Resources Research*. Wageningen University. Retrieved from <http://library.wur.nl/WebQuery/wdab/1861424>
- Leijnse, H., Uijlenhoet, R., & Stricker, J. N. M. (2007a). Hydrometeorological Application Of A Microwave Link: 2. Precipitation. *Water Resources Research*, 43(4), 1–9. doi:10.1029/2006WR004989
- Leijnse, H., Uijlenhoet, R., & Stricker, J. N. M. (2007b). Rainfall Measurement Using Radio Links From Cellular Communication Networks. *Water Resources Research*, 43(3). doi:10.1029/2006WR005631

- Leijnse, H., Uijlenhoet, R., & Stricker, J. N. M. (2008). Microwave Link Rainfall Estimation: Effects Of Link Length And Frequency, Temporal Sampling, Power Resolution, and Wet Antenna Attenuation. *Advances in Water Resources*, 31(11), 1481–1493.
doi:10.1016/j.advwatres.2008.03.004
- Lensky, I. M., & Rosenfeld, D. (2005). The time-space exchangeability of satellite retrieved relations between cloud top temperature and particle effective radius. *Atmospheric Chemistry and Physics Discussions*, 5(6), 11911–11928. doi:10.5194/acpd-5-11911-2005
- Messer, H., Goldshtein, O., Rayitsfeld, A., & Alpert, P. (2008). Recent results of rainfall mapping from cellular network measurements. *2008 IEEE International Conference on Acoustics, Speech and Signal Processing*, (1), 5157–5160. doi:10.1109/ICASSP.2008.4518820
- Messer, H., Zinevich, A., & Alpert, P. (2012). Environmental Sensor Networks Using Existing Wireless Communication Systems For Rainfall And Wind Velocity Measurements. In *IEEE Instrumentation & Measurement Magazine* (Vol. 15, pp. 32–38). doi:10.1109/MIM.2012.6174577
- Moseley, C., Berg, P., & Haerter, J. O. (2013). Probing the precipitation life cycle by iterative rain cell tracking. *Journal of Geophysical Research: Atmospheres*, 118(24), 13361–13370.
doi:10.1002/2013JD020868
- Olsen, R. L., Rogers, D. V., & Hodge, D. B. (1978). The aRb Relation in the Calculation of Rain Attenuation. *IEEE Transactions on Antennas and Propagation*, 26(2), 318–329.
doi:10.1109/TAP.1978.1141845
- Ostrometzky, J., & Messer, H. (2014). Accumulated Rainfall Estimation Using Maximum Attenuation Of Microwave Radio Signal. In *2014 IEEE 8th Sensor Array and Multichannel Signal Processing Workshop (SAM)* (pp. 193–196). IEEE. doi:10.1109/SAM.2014.6882373
- Overeem, A., Leijnse, H., & Uijlenhoet, R. (2011). Measuring Urban Rainfall Using Microwave Links From Commercial Cellular Communication Networks. *Water Resources Research*, 47(12), 1–16. doi:10.1029/2010WR010350
- Overeem, A., Leijnse, H., & Uijlenhoet, R. (2013a). Country-wide Rainfall Maps From Cellular Communication Networks. *Proceedings of the National Academy of Sciences of the United States of America*, 110(8), 2741–5. doi:10.1073/pnas.1217961110
- Overeem, A., Leijnse, H., & Uijlenhoet, R. (2013b). Country-wide rainfall maps from cellular communication networks. *Proceedings of the National Academy of Sciences of the United States of America*, 110(8), 2741–5. doi:10.1073/pnas.1217961110
- Perlman, H. (2014). The Water Cycle. Retrieved June 3, 2015, from
<http://water.usgs.gov/edu/watercycle.html>
- Perlman, H. (2015). Precipitation: The Water Cycle. Retrieved June 3, 2015, from
<http://water.usgs.gov/edu/watercycleprecipitation.html>

- Rahim, S. K. A., Rahman, T. A., Tan, K. G., & Reza, A. W. (2012). Microwave Signal Attenuation Over Terrestrial Link At 26 GHz In Malaysia. *Wireless Personal Communications*, 67(3), 647–664. doi:10.1007/s11277-011-0402-8
- Rientjes, T. H. M., & Alemseged, T. H. (2007). Spatio-Temporal Rainfall Mapping From Space : Setbacks and strengths. In *5th International Symposium on Spatial Data Quality: Modelling Qualities in Space and Time* (pp. 1–9). Enschede, Netherlands: Int. Inst. for Geo-Info and Earth Obs. Retrieved January 25,2016, from <http://www.isprs.org/proceedings/XXXVI/2-C43/Session1/alemseged.pdf>
- Rincon, R. F., & Lang, R. H. (2002). Microwave link dual-wavelength measurements of path-average attenuation for the estimation of drop size distributions and rainfall. *IEEE Transactions on Geoscience and Remote Sensing*, 40(4), 760–770. doi:10.1109/TGRS.2002.1006324
- Roebeling, R. A., & Holleman, I. (2009). SEVIRI rainfall retrieval and validation using weather radar observations. *Journal of Geophysical Research: Atmospheres*, 114(21), 1–13. doi:10.1029/2009JD012102
- Rosenfeld, D. (2007). Cloud top microphysics as a tool for precipitation measurements. In V. Levizzani, P. Bauer, & F. J. Turk (Eds.), *Measuring Precipitation From Space* (Vol. 1, pp. 61–77). Dordrecht: Springer. doi:10.1007/978-1-4020-5835-6_6
- Rosenfeld, D., & Gutman, G. (1994). Retrieving microphysical properties near the tops of potential rain clouds by multispectral analysis of AVHRR data. *Atmospheric Research*, 34(1-4), 259–283. doi:10.1016/0169-8095(94)90096-5
- Rosow, W. B., & Schiffer, R. A. (1999). Advances in Understanding Clouds from ISCCP. *Bull. Amer. Meteor. Soc.*, 80(11), 2261–2287. doi:10.1175/1520-0477(1999)080<2261:AIUCFI>2.0.CO;2
- Schleiss, M., & Berne, A. (2010). Identification of dry and rainy periods using telecommunication microwave links. *IEEE Geoscience and Remote Sensing Letters*, 7(3), 611–615. doi:10.1109/LGRS.2010.2043052
- Schmetz, J., Pili, P., Tjemkes, S., Just, D., Kerkmann, J., Rota, S., & Ratier, A. (2002). An introduction to Meteosat Second Generation (MSG). *Bulletin of the American Meteorological Society*, 83(7), 977–992. doi:10.1175/1520-0477(2002)083<0977:AITMSG>2.3.CO;2
- Scofield, R. A. (1987). The NESDIS Operational Convective Precipitation- Estimation Technique. *Monthly Weather Review*, 115(8), 1773–1793. doi:10.1175/1520-0493(1987)115<1773:TNOCP>2.0.CO;2
- Semplak, R. A., & Turrin, R. H. (1969). Some measurements of attenuation by rainfall at 18.5 {GHz}. *Bell System Technical Journal*, 48(6), 1767–1772. doi:10.1002/j.1538-7305.1969.tb01151.x

- Simpson, J. (2003). *Cloud Systems, Hurricanes, and the Tropical Rainfall Measuring Mission (TRMM)*. (W.-K. Tao & R. Adler, Eds.) (1st editio.). Boston, MA: American Meteorological Society. doi:DOI 10.1007/978-1-878220-63-9
- Strangeways, I. (2006). *Precipitation: Theory, Measurement and Distribution/Cambridge*. New York: Cambridge University Press.
- The Problem of Parallax. (2006). Retrieved February 22, 2016, from <http://cimss.ssec.wisc.edu/goes/blog/archives/217>
- Thies, B., Nauß, T., & Bendix, J. (2008). Precipitation process and rainfall intensity differentiation using Meteosat Second Generation Spinning Enhanced Visible and Infrared Imager data. *Journal of Geophysical Research*, 113(D23), D23206. doi:10.1029/2008JD010464
- Thomas, C., Corpetti, T., & Mémin, E. (2009). Data assimilation for convective cells tracking in MSG images. In *Geoscience and Remote Sensing Symposium, 2009 IEEE International, IGARSS 2009* (Vol. 2, pp. 1–5). Cape Town: IEEE. doi:10.1109/IGARSS.2009.5418217
- Townsend, A. J., & Watson, R. J. (2011). The linear relationship between attenuation and average rainfall rate for terrestrial links. *IEEE Transactions on Antennas and Propagation*, 59(3), 994–1002. doi:10.1109/TAP.2010.2103021
- Vicente, G. A., Scofield, R. A., & Menzel, W. P. (1998). The Operational GOES Infrared Rainfall Estimation Technique. *Bulletin of the American Meteorological Society*, 79(9), 1883–1898. doi:10.1175/1520-0477(1998)079<1883:TOGIRE>2.0.CO;2
- Wang, Z., Schleiss, M., Jaffrain, J., Berne, A., & Rieckermann, J. (2012). Using markov switching models to infer dry and rainy periods from telecommunication microwave link signals. *Atmospheric Measurement Techniques*, 5(7), 1847–1859. doi:10.5194/amt-5-1847-2012
- Woodley, W. L., Jordan, J., Barnston, A., Simpson, J., Biondini, R., & Flueck, J. (1982). Rainfall Results of the Florida Area Cumulus Experiment, 1970–76. *Journal of Applied Meteorology*, 21(2), 139–164. doi:10.1175/1520-0450(1982)021<0139:RROTFA>2.0.CO;2
- Young, A. H., Bates, J. J., & Curry, J. A. (2013). Application of cloud vertical structure from CloudSat to investigate MODIS-derived cloud properties of cirriform, anvil, and deep convective clouds. *Journal of Geophysical Research: Atmospheres*, 118(10), 4689–4699. doi:10.1002/jgrd.50306
- Zinevich, A., Messer, H., & Alpert, P. (2010). Prediction of rainfall intensity measurement errors using commercial microwave communication links. *Atmospheric Measurement Techniques*, 3(5), 1385–1402. doi:10.5194/amt-3-1385-2010

APPENDIX

Appendix 1: Wet/dry classification and estimating reference signal for observation on 11-05-2013

Time	MRSL	Me_RSL	mRSL	LSD	VAR	Mean	Ref
5:00	-37.1	-37.35	-37.7	0.105409	0.011111	-37.6	-38.1
5:15	-36.9	-37.3	-37.5				
5:30	-37	-37.34	-37.5				
5:45	-37	-37.37	-37.5				
6:00	-37	-37.35	-37.5				
6:15	-37	-37.36	-37.5				
6:30	-37	-37.35	-37.7				
6:45	-37.2	-37.34	-37.7				
7:00	-37.1	-37.35	-37.7				
7:15	-37.2	-37.39	-37.7				
7:30	-37.1	-37.37	-37.7	0.113529	0.012889	-37.58	-37.6
7:45	-37	-37.34	-37.6				
8:00	-37	-37.3	-37.5				
8:15	-37	-37.33	-37.5				
8:30	-37.1	-37.32	-37.5				
8:45	-36.9	-37.34	-37.5				
9:00	-36.9	-37.28	-37.5				
9:15	-37	-37.31	-37.5				
9:30	-37	-37.36	-37.7				
9:45	-37.1	-37.4	-37.8				
10:00	-37.4	-38.1	-38.6	4.363026	19.036	-43.44	-37.58
10:15	-37.3	-38.08	-45.1				
10:30	-44.5	-46.81	-49.1				
10:45	-41.4	-43.65	-49.3				
11:00	-40.6	-44.5	-49.3				
11:15	-39.7	-40.62	-41.6				
11:30	-39.1	-39.59	-40.3				
11:45	-38.7	-39.3	-40				
12:00	-38.7	-40.17	-41.7				
12:15	-38.2	-38.78	-39.4				
12:30	-38.9	-39.97	-40.8	1.6043	2.573778	-39.46	
12:45	-39.9	-40.44	-41				
13:00	-39.9	-40.82	-42.5				
13:15	-38.5	-39.55	-40.5				
13:30	-38	-38.43	-38.9				
13:45	-37.9	-38.09	-38.4				
14:00	-37.6	-37.94	-38.4				
14:15	-37.5	-37.69	-38.1				
14:30	-37.5	-37.65	-38				
14:45	-37.5	-37.67	-38				
15:00	-37.5	-37.68	-37.9	0.048305	0.002333	-37.93	
15:15	-37.5	-37.67	-37.9				
15:30	-37.5	-37.67	-37.9				
15:45	-37.5	-37.67	-37.9				
16:00	-37.5	-37.65	-37.9				
16:15	-37.4	-37.64	-37.9				
16:30	-37.5	-37.61	-37.9				
16:45	-37.5	-37.62	-38				
17:00	-37.5	-37.63	-38				
17:15	-37.5	-37.62	-38				
17:30	-37.4	-37.63	-38	0.113529	0.012889	-37.82	
17:45	-37.4	-37.63	-38				
18:00	-37.3	-37.6	-37.9				
18:15	-37.1	-37.48	-37.8				
18:30	-37.1	-37.45	-37.8				
18:45	-37.2	-37.43	-37.7				
19:00	-37.2	-37.44	-37.7				
19:15	-37.2	-37.49	-37.7				
19:30	-37.2	-37.51	-37.8				
19:45	-37.3	-37.57	-37.8				
20:00	-37.3	-37.53	-37.9	0.067495	0.004556	-37.77	

Where MRSL is maximum RSL, Me_RSL is mean RSL and mRSL is minimum RSL, LSD is standard deviation, VAR is variance and Ref is reference signal level

The figure above is a snap shot of part of the data used in study for the period 11th May 2013. In this study, wet and dry classification are performed using the approach illustrated by Schleiss & Berne (2010) coupled with PAR from rain gauges under link transect. Per the approach of Schleiss & Berne (2010), statistical values for variance and standard deviation are calculated every 2 hours 30 minutes using the mRSLs. The time series statistical information for the signal level is compared with each other and to PAR observation to verify it corresponds with it. By this, wet periods could be separated from dry periods.

Eventually, baseline signal level is estimated as an average of 10 periods preceding the identified wet period.

Appendix 2: Deriving rainfall based on power law relation

From $A = aR^b$

$$R = \left(\frac{A}{a}\right)^{\frac{1}{b}}$$

But attenuation, A, above is estimated as $A = \frac{Ref - mRSL}{L}$

Where L is link length (3.68km)

For each of the periods categorized as wet period, as illustrated in appendix 1, R would be estimated based on equation above.

Example

In appendix 1 above, yellow cell is dry period and orange cells are wet period

For first cell in wet period; R would be estimated as follows (using ITU coefficients; a=0.05008 and b=1.044)

$$A = \frac{-37.58 - (-38.6)}{3.86}$$

$$A = 0.264$$

$$R = \left(\frac{0.264}{0.05008}\right)^{\frac{1}{1.044}}$$

$$R = 4.915\text{mm/h}$$

Appendix 3: Estimating wet antenna correction factor

Correction factors are derived on the basis of overestimation due to wet antenna for each of different coefficient used in modelling rainfall. Peak rain intensities for both modelled (due to wet antenna attenuation) and observed from PAR are illustrated in table below

Coefficient	Peak PAR (mm/h)	Peak modelled R due to wet antenna attenuation (mm/h)
ITU	31.8	53.4
JT	31.8	62.2
LP	31.8	51.4

The factor is derived by computing the difference between the modelled and observed rain rates divided by their sum.

For ITU:
$$A_w = \frac{53.4-31.8}{53.4+31.8}$$

$$= 0.25$$

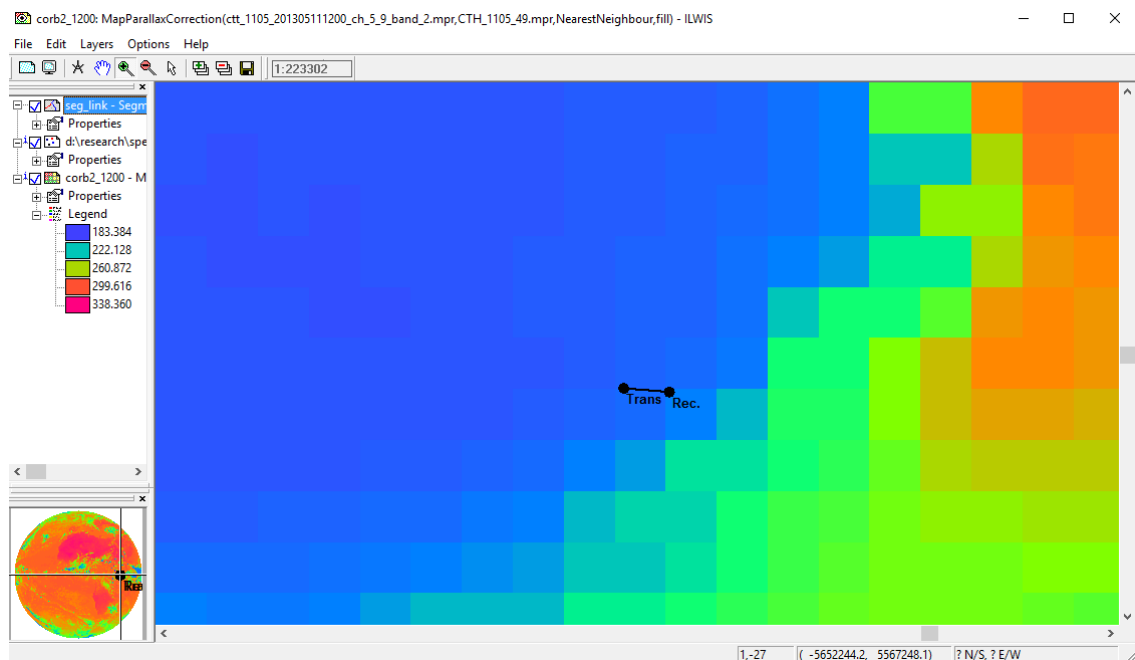
For LP:
$$A_w = \frac{51.4-31.8}{51.4+31.8}$$

$$= 0.23$$

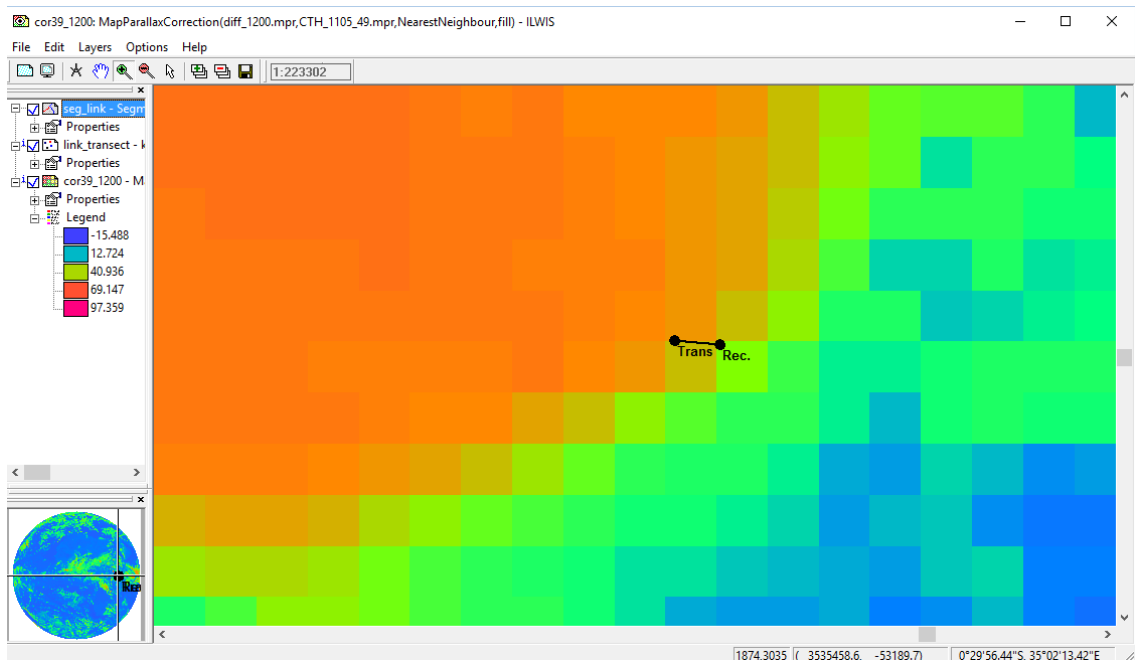
For JT:
$$A_w = \frac{62.2-31.8}{62.2+31.8}$$

$$= 0.32$$

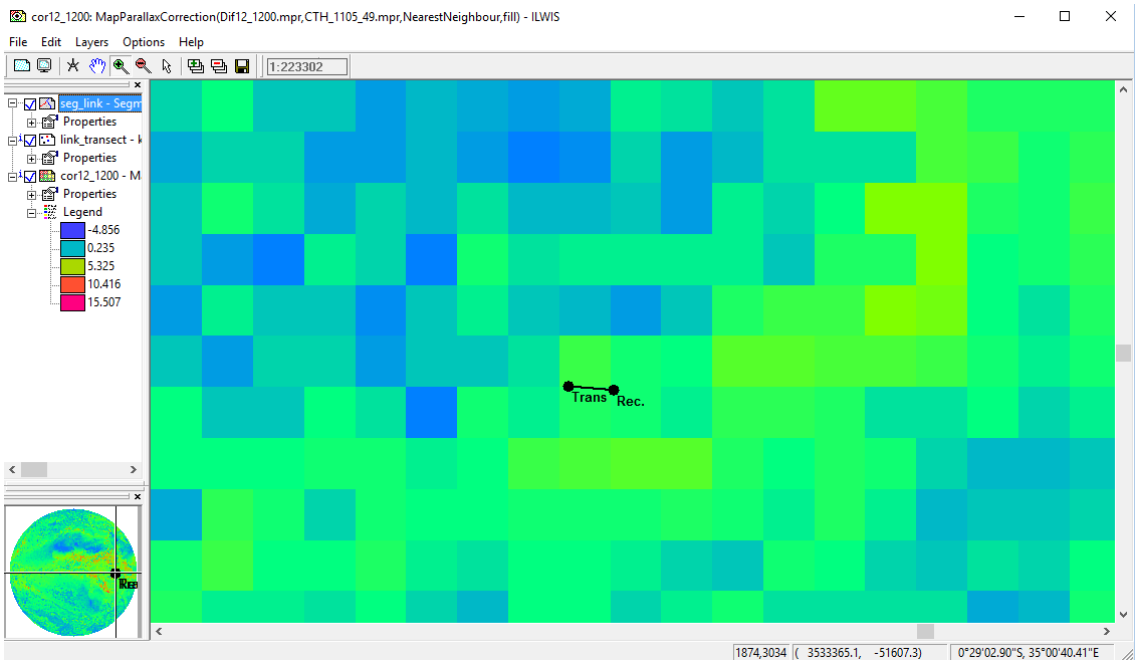
Appendix 4: Cloud microphysical properties retrieved on 11th May 2013, 12:00 PM



Cloud top temperature based on MSG IR 10.8 micron channel
CTT increases from blue to pink in images



Cloud effective radius (CRE)
CRE increases from blue to pink in image

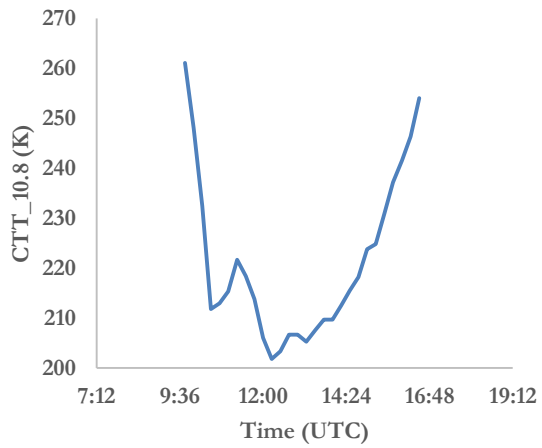


Cloud optical thickness (COT)
Optical thickness increases from blue to pink in image. In all three images, two black dots joined with a line is the link transect, Trans is transmitting antenna and Rec is receiving antenna.

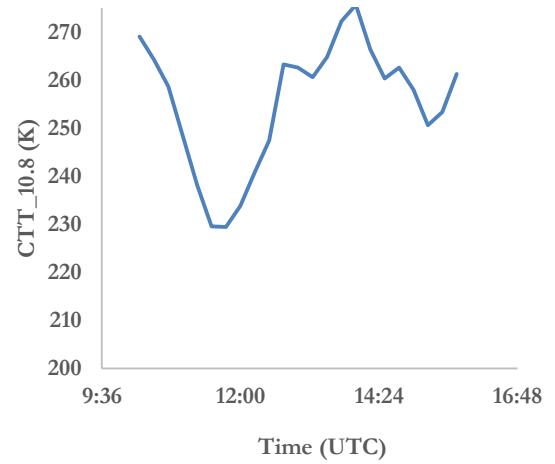
Note: although cloud tops are cold and drops are larger, cloud is optically thing with respect to the thresholds for possibility of occurrence of rain.

All images are parallax corrected

Appendix: 5 Thermal profiles of cloud cover for the experimental period



(a) Thermal profile for 11th May 2013



(b) Thermal profile for 12th May 2013

Appendix 5 compares the thermal profile for the two periods: 11th May 2013 and 12th May 2013 considered. It can be seen that the cloud cover for 12th May analysis was comparatively lower, as such might explain the differences in rainfall intensities observed for the two periods. Also, as has been indicated in literature, the cloud microphysical composition of this cloud might also be significantly different (but however parameterized based on the same assumptions as for 11th May analysis) and there by resulting in the weak relationship it has with the ground observation from MW link